RSC Medicinal Chemistry

ROYAL SOCIETY OF CHEMISTRY

RESEARCH ARTICLE

Cite this: *RSC Med. Chem.*, 2023, **14**, 2714

New nitazoxanide derivatives: design, synthesis, biological evaluation, and molecular docking studies as antibacterial and antimycobacterial agents†

Mahmoud Saleh,[a] Yaser A. Mostafa, ‡[a] Jyothi Kumari,[b] Momen M. Thabet,[c] Dharmarajan Sriram,[b] Mahmoud Kandeel[de] and Hajjaj H. M. Abdu-Allah *[a]

Received 29th August 2023,
Accepted 5th October 2023

DOI: 10.1039/d3md00449j

rsc.li/medchem

A new series inspired by combining fragments from nitazoxanide (NTZ) and 4-aminosalicylic acid (4-ASA) was synthesized and screened for *in vitro* antibacterial and antimycobacterial activities. The majority showed higher antibacterial potency than NTZ against all the screened strains, notably, **5f**, **5j**, **5n** and **5o** with MICs of 0.87–9.00 μM. Compounds **5c**, **5n** and **5o** revealed higher potency than ciprofloxacin against *K. pneumoniae*, while **5i** was equipotent. For *E. faecalis*, **3b**, **5j**, and **5k** showed higher potency than ciprofloxacin. **5j** was more potent against *P. aeruginosa* than ciprofloxacin, while **5n** was more potent against *S. aureus* with an MIC of 0.87 μM. **5f** showed equipotency to ciprofloxacin against *H. pylori* with an MIC of 1.74 μM. Compounds **3a** and **3b** (4-azidoNTZ, MIC 4.47 μM) are 2 and 5-fold more potent against *Mycobacterium tuberculosis* (Mtb H_{37}Rv) than NTZ (MIC 20.23 μM) and safer. 4-Azidation and/or acetylation of NTZ improve both activities, while introducing 1,2,3-triazoles improves the antibacterial activity. Molecular docking studies within pyruvate ferredoxin oxidoreductase (PFOR), glucosamine-6-phosphate synthase (G6PS) and dihydrofolate reductase (DHFR) active sites were performed to explore the possible molecular mechanisms of actions. Acceptable drug-likeness properties were found. This study may shed light on further rational design of substituted NTZ as broad-spectrum more potent antimicrobial candidates.

1. Introduction

Infectious diseases pose a significant global health challenge, underscoring the ongoing requirement for research and advancement in the domain of anti-infective medications.[1–4] The COVID-19 pandemic has heightened awareness about the peril presented by infectious diseases and has become a prime driving force for revitalizing endeavors to combat the latent crisis of antibiotic-resistant bacteria.[5] Notably, there is a rising trend of resistance among ESKAPE pathogens (*Enterococcus faecium*, *Staphylococcus aureus*, *Klebsiella pneumoniae*, *Acinetobacter baumannii*, *Pseudomonas aeruginosa*, and *Enterobacter* spp.) and *Escherichia coli* against multiple antibiotic classes, resulting in the deterioration of once manageable infections.[6] Tuberculosis (TB), an exceedingly contagious, life-threatening, and challenging-to-treat bacterial infection, serves as another illustration. The World Health Organization (WHO) identifies TB as the primary cause of death attributed to a single infectious agent.[7] Isoniazid, pyrazinamide, rifampicin, and ethambutol are the first-line antitubercular agents, while second-line options like streptomycin, fluoroquinolones, bedaquiline, and 4-aminosalicylic acid (4-ASA) are reserved for drug-resistant cases.[8] Beside the complex, lengthy treatment to manage drug-sensitive cases, the main concerns lie in multidrug-resistant TB (MDR-TB) and extensive drug-resistant TB (XDR-TB), which result in treatment failure.[8] Counteracting antibiotic resistance mandates the development of potent novel antimycobacterial drugs possessing increased efficacy, devoid of cross-resistance to established drugs, lowered toxicity, and enhanced cell permeability.[9] Therefore, there is an urgent need for the discovery of safer and more effective new drugs with novel mechanisms of action for the treatment

[a] *Pharmaceutical Organic Chemistry Department, Faculty of Pharmacy, Assiut University, Assiut 71526, Egypt. E-mail: hajjaj@aun.edu.eg*
[b] *Department of Pharmacy, Birla Institute of Technology & Science-Pilani, Hyderabad Campus, Jawahar Nagar, Hyderabad-500 078, India*
[c] *Microbiology and Immunology Department, Faculty of Pharmacy, South Valley University, Qena 83523, Egypt*
[d] *Department of Biomedical Sciences, College of Veterinary Medicine, King Faisal University, 31982 Al-Ahsa, Saudi Arabia*
[e] *Department of Pharmacology, Faculty of Veterinary Medicine, Kafrelsheikh University, 33516 Kafrelsheikh, Egypt*
† Electronic supplementary information (ESI) available. See DOI: https://doi.org/10.1039/d3md00449j
‡ Current address: Pharmaceutical Chemistry Department, Faculty of Pharmacy, Badr University in Assiut, Assiut 71511, Egypt.

of TB. One of the strategies to gain an effective therapy against drug-resistant infectious diseases is based on the hybridization of different pharmacophores binding diverse biomolecular targets. This tactic holds the potential to yield versatile, wide-spectrum antimicrobial agents targeting multiple facets.[10] Salicylanilides, such as niclosamide (Fig. 1), have displayed extensive antimicrobial properties against helminths, fungi, protozoa, mycobacteria, bacteria, and viruses, employing a variety of mechanisms.[11–16] On the other hand, 5-nitrothiazoles such as niridazole, nitazoxanide (NTZ) and tizoxanide (TIZ) (Fig. 1) display potent antimicrobial and anthelmintic activities.[17,18] These agents have been demonstrated to inhibit enzymatic activities involved in energy metabolism[19,20] and to be reduced into adduct forming metabolites.[21–23] Interestingly, the two new clinically used antiTB drugs delamanid and pretomanid (Fig. 1) are nitroimidazoles.[24]

A structural analogue of the antimicrobial agent niclosamide, nitazoxanide (NTZ, Fig. 1), was prepared by substituting a nitrothiazolyl amide moiety for the anilide group in the original compound.[25] NTZ has broad-spectrum anthelmintic,[26–28] antiparasitic,[25–29] antibacterial,[30] and antiviral[31,32] activities. However, NTZ is almost completely ineffective against aerobically grown *Staphylococcus*, *Enterococcus*, *Pseudomonas* and *Enterobacteriaceae*.[30] Interestingly, both replicating and nonreplicating Mtb are efficiently eradicated by NTZ[33] through the disruption of the Mtb membrane potential and intrabacterial pH homeostasis.[34] NTZ is a prodrug that is rapidly hydrolyzed in the body into its active metabolite tizoxanide (TIZ)[35,36] which disrupts anaerobic energy metabolism *via* inhibition of pyruvate ferredoxin oxidoreductase (PFOR).[37] Thus, NTZ has a lower risk of inducing mutation-based drug-resistance.[37] Also, nitroreductase inhibition and peptide disulfide isomerase inhibition are two other proposed modes of activity through which NTZ exerts its biological activity.[38–40] NTZ is distinct for its several modes of action,[34] being non-toxic and the absence of reported microbial resistance.[34,38] Modification of the nitrothiazole, salicylyl and the amidic linker was carried out to explore the structure–activity relationship of NTZ as an antimicrobial agent.[41–43] These modifications indicate that the 5-nitro group is important for antimicrobial activity, while the salicylyl moiety modifications are well-tolerated. NTZ is therefore a suitable template to inspire the identification and development of novel broad-spectrum anti-infective agents. On the other hand, 4-aminosalicylic acid (4-ASA) is a second line antiTB medication.[44] It is known for having low absorption, quick metabolism and elimination, necessitating high daily doses of up to 12 g per day, which causes several side effects including gastrointestinal problems.[45] To increase its metabolic stability and activity, 4-ASA has its carboxylic and 4-amino groups undergone structural modification strategies.[46–50] One of these strategies is to employ 4-azidosalicylic acid as a precursor for 4-ASA because it is anticipated that mycobacteria will bioreductively activate it.[50] The azido group is also an active moiety in some biologically active compounds such as anti-TB[51] (compound **I**; Fig. 1) and zidovudine, a clinically used antiviral drug.[52] Moreover, the antibacterial and antiprotozoal properties of the broad-spectrum antibiotic metronidazole were significantly enhanced by converting its hydroxyl group into azide (compound **II**; Fig. 1).[53] Currently, the azido group is most frequently used in the field of click cycloaddition reactions to introduce the 1,4-disubstituted-1,2,3-triazole moiety (compound **III**; Fig. 1) in order to enhance the solubility and/or biological activities of antimicrobial agents,[54–57] particularly, antiTB compounds.[49,58–60] The above-mentioned information emphasizes the resourceful importance of both NTZ and 4-ASA in antimicrobial and antitubercular activities. This inspired us to integrate the two drugs' structural components into a single hybrid molecule through the triazole ring (Fig. 2), aiming to develop multitarget broad-spectrum antimicrobial agents that hopefully could bypass resistance. To achieve this goal, 4-ASA

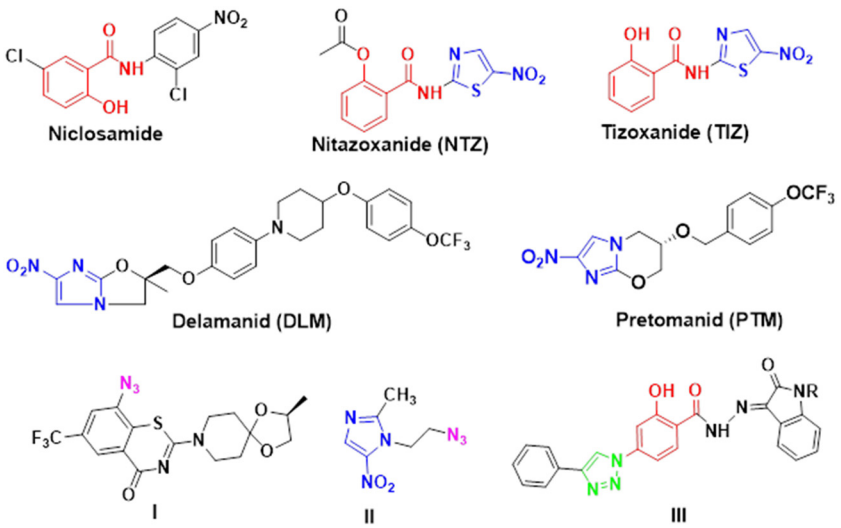

Fig. 1 Structures of NTZ and some related antimicrobial compounds.

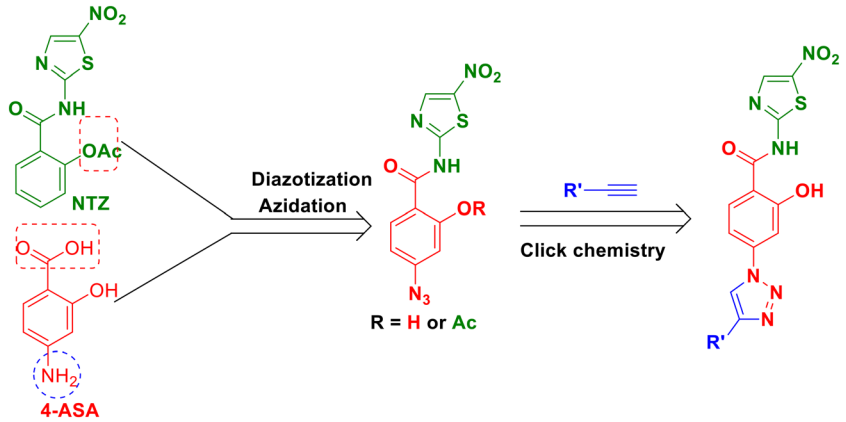

Fig. 2 Target molecule design strategy. The chemical structures of nitazoxanide (NTZ) and 4-aminosalicylic acid (4-ASA); general structures of the title compounds. For R^- refer to Scheme 1.

was converted into 4-azidosalicylic acid that was amidated with 2-amino-5-nitrothiazole and then the click reaction provided 1,2,3-triazole derivatives appended with common antimicrobial pharmacophores (piperidine, piperazine, morpholine, isatin and benzothiazole).[61,62] These compounds were *in vitro* screened for their antibacterial and mycobacterial activities.

2. Results and discussion

2.1. Chemistry

The target compounds (**3a**, **3b** and **5a–5q**) were synthesized as described in Scheme 1. 4-Azidosalicylic acid (**2**) was obtained in 87% yield by diazotization of 4-ASA and then azidation.[63] For the synthesis of amide **3a**, **2** was converted into acid chloride by reaction with thionyl chloride in the presence of a catalytic amount of DMF. The reaction of this acid chloride with 2-amino-5-nitrothiazole in the presence of triethylamine gave a semisolid tarry product that was difficult to purify. Instead, **3a** was successfully synthesized in high yield (77%) and without the need for column purification by coupling **2** with 2-amino-5-nitrothiazole employing *N*,*N*′-carbonyldiimidazole (CDI) as an amide coupling reagent. **3a** was characterized by the appearance of an azide peak at 2100 cm^{-1} and an amidic carbonyl band at 1666 cm^{-1} in the IR spectrum and the ^{1}H-NMR spectrum showed a singlet at δ 8.51 ppm integrating for one proton corresponding to amidic NH, a singlet at δ 8.97 corresponding to the thiazole ring proton and a broad singlet at δ 14.22 ppm corresponding to phenolic OH. Compound **3a** was acetylated by reaction with acetic anhydride in the presence of a catalytic amount of conc. H_2SO_4 to give **3b** in 71% yield. The structure of **3b** was confirmed by the appearance of a peak at 1765 cm^{-1} in IR for acetyl carbonyl and the appearance of an NMR signal at 2.25 ppm for acetyl CH_3.

For the synthesis of the final target compounds, two pathways were envisioned. The first was to react **3a** with propargyl bromide to provide the key intermediate bromomethyl-1,2,3-triazole derivative (Scheme 2) that could be used for alkylation of *N* or *S* nucleophiles. Surprisingly, the click reaction between **3a** and propargyl bromide was unsuccessful even after several trials and under different reaction conditions such as using different solvents (THF, *tert*-butanol or DMF) with or without H_2O, different temperatures, different reaction times and/or different ratios of $CuSO_4$/sodium ascorbate. Under these different reaction conditions, the starting material was isolated without undergoing any change as confirmed by the physical and spectral data. This excluded the possibility of any side reaction.

The second pathway involved propargylation of the appropriate cyclic amine, 2-mercaptobenzothiazole or isatin derivative in the presence of potassium carbonate and DMF (Scheme 1) and afforded the propargylated derivatives (**4f–4q**) in 76–83% yield.[64–70] Finally, the target 1,2,3-triazoles (**5a–5q**) were obtained in 76–89% yield *via* Cu-catalyzed click cycloaddition of **3a** with the alkyne or propargylated derivatives (**4f–q**) under standard conditions. All **5a–q** were fully characterized using IR, ^{1}H-NMR, ^{13}C-NMR, ESI-MS and elemental analyses. In common, two characteristic singlet signals corresponding to the thiazole ring proton at 8.68–9.50 ppm and the triazole ring proton at 7.49–8.73 ppm were found in ^{1}H-NMR of all synthesized compounds (**5a–5q**).

2.2. Biological evaluation

2.2.1. *In vitro* antibacterial activity. Compounds **3a**, **3b**, and **5a–5q** were screened for their *in vitro* antibacterial activity against six different bacterial strains: *S. aureus* ATCC 6538 and *E. faecalis* ATCC 19433 as Gram-positive wild-type strains, *E. coli* ATCC 8739, *P. aeruginosa* ATCC 27853, and *K. pneumoniae* ATCC 10031 as Gram-negative wild-type strains and *H. pylori* ATCC 700392 as an anaerobe, by a broth micro-dilution method. The minimum inhibitory concentration (MIC) screening data of the synthesized compounds along with NTZ and ciprofloxacin as a standard drug for comparison are listed in Table 1. The synthesized compounds revealed high potency and a broad spectrum of activity against the Gram-positive, Gram-negative and anaerobic bacteria with varying MIC values according to bacterial strains. The compounds **3a**, **5c**, **5o** and

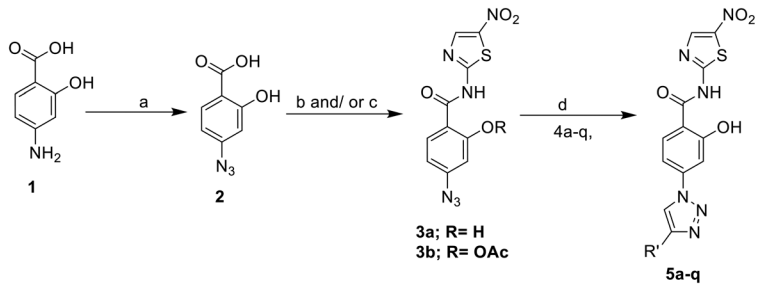

Compd No.	R'	Compd No.	R'	Compd No.	R'
5a	CH_2OH	5g		5m	
5b	COOH	5h		5n	
5c	$COOCH_3$	5i		5o	
5d		5j		5p	
5e		5k		5q	
5f		5l			

Scheme 1 Reagent and conditions: (a) (i) $NaNO_2$, H_2SO_4, 0 °C, 3 h, (ii) NaN_3, 19 h, 87%; (b) (i) CDI, THF, reflux, 3 h, (ii) 2-amino-5-nitrothiazole, reflux, 6 h, 77%; (c) Ac_2O, conc. H_2SO_4, 60 °C, 1 h, 71%; (d) appropriate alkyne/propargylated derivatives, $CuSO_4{\cdot}5H_2O$, Na ascorbate, THF/H_2O, rt, 2–4 h,76–89%.

5q with MICs of 1.48–4.89 μM are about 20-fold more potent than the parent NTZ (MIC = 104.13 μM) against *E. coli*. Among them, **5o** was the most promising with an MIC of 1.48 μM, while that of ciprofloxacin is 0.3 μM. Interestingly, the compounds **5g**, **5j**, **5l** and **5n** with MICs of 2.96–7.91 μM are about 50-fold more potent than the parent NTZ (MIC = 416.55 μM) against *P. aeruginosa*. Compound **5j** was the most promising with an MIC of 2.96 μM. Two compounds, **5j** showed higher potency than ciprofloxacin (MIC 4.53 μM), while **5n** is equipotent. Furthermore, the sensitivity of *K. pneumoniae* to the synthesized compounds **5c**, **5i**, **5n** and **5o** with MICs of 3.95–8.99 μM is up to 20-fold higher than that to the parent NTZ (MIC = 182.24 μM). Compounds **5c**, **5n** and **5o** with MICs of 5.12, 4.38 and 3.95 μM, respectively, are more potent than ciprofloxacin (MIC 9.05 μM), while **5i** is equipotent. Concerning the activity against *S. aureus*, it's worth mentioning that the sensitivity to the compounds **5g**, **5h**, **5i**, **5n** and **5q** with MICs of 0.87–6.95 μM is 25-fold higher than that to the parent NTZ (MIC = 104.13 μM). Compound **5n** was the most promising with an MIC of 0.87 μM, which is more potent than ciprofloxacin (MIC 3.01 μM), while **5g** and **5q** are equipotent. Interestingly, the sensitivity of *E. faecalis* to the synthesized compounds **3b**, **5j**, **5k**, **5l**, and **5o** with MICs of 1.97–5.93 μM is 25-fold more potent than that to the parent NTZ (MIC = 156.20

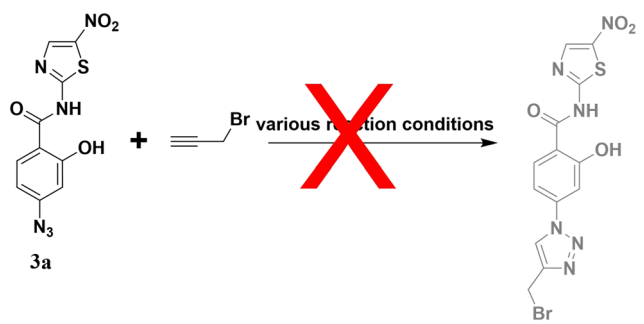

Scheme 2 Attempts to prepare the bromomethylated triazole derivative of **3a**.

Table 1 Antibacterial activity against different bacterial strains (MIC in μM)[a]

	Gram-negative strains			Gram-positive strains		Anaerobe strain
ID	*E. coli* ATCC 8739	*P. aeruginosa* ATCC 27853	*K. pneumoniae* ATCC 10031	*S. aureus* ATCC 6538	*E. faecalis* ATCC 19433	*H. pylori* ATCC 700392
3a	4.89	—	313.46	9.79	26.12	104.48
3b	8.61	91.87	34.45	11.48	2.15	11.48
5a	—	353.27	88.31	—	132.47	44.15
5b	6.64	10.62	15.94	85.03	—	21.25
5c	3.84	15.37	5.12	10.24	—	3.84
5d	—	—	39.17	29.38	19.58	14.69
5e	7.10	303.01	—	1212.07	75.75	5.91
5f	74.51	—	1192.21	9.31	27.94	1.74
5g	6.01	7.22	12.03	3.61	—	19.25
5h	1186.76	148.34	18.54	6.95	—	9.27
5i	—	143.99	8.99	4.49	—	6.74
5j	11.84	2.96	252.669	505.39	1.97	31.58
5k	—	16.27	—	32.55	4.06	130.23
5l	—	7.85	—	15.70	4.90	3.92
5m	486.80	—	60.85	—	—	4.75
5n	21.04	5.26	4.38	0.87	8.76	3.50
5o	1.48	7.91	3.95	506.46	5.93	2.96
5p	15.34	—	490.92	92.04	184.09	9.58
5q	3.90	31.27	23.45	3.90	—	15.63
TIZ	180.96	361.93	241.29	150.80	135.72	11.31
NTZ	104.13	416.55	182.24	104.13	156.20	13.01
Ciprofloxacin	0.30	4.53	9.05	3.01	6.03	1.50

[a] Values are means of three experiments.

μM). The compounds **3b**, **5j** and **5k** with MICs of 2.15, 1.97 and 4.06 μM, respectively, are more potent than ciprofloxacin (MIC 6.03 μM), while **5l** is equipotent. Moreover, among the synthesized compounds **5e**, **5f**, **5l**, **5m**, **5n**, **5o** and **5p** with MICs of 1.74–5.91 μM are more potent than NTZ (MIC = 13.01 μM) against *H. pylori*. Compound **5f** (MIC = 1.74 μM) is equipotent to ciprofloxacin (MIC 1.5 μM). The results clearly show that introducing a 1,2,3-triazole ring at the 4-position of the NTZ phenyl tail improved the activity significantly and provided compounds with a broader spectrum and higher potency. Some compounds are even more potent than ciprofloxacin, particularly, against *S. aureus*, *E. faecalis*, and *P. aeruginosa*. The heterocyclic moieties linked to the triazole ring contribute positively to the activity, particularly, 5-haloisatins (**5l–5n**), 5-methylisatin (**5o**), benzothiazole (**5q**) and *N*-phenylpiperazine (**5j**). In contrast, the activity of this series of compounds is adversely affected by the presence of polar groups such as OH (**5a**) or COOH (**5b**) linked to the triazole ring.

Accordingly, the study revealed that compounds **5f**, **5j**, **5n** and **5o** are the most potent antibacterial agents and exhibit a broad spectrum of activity against Gram-positive and Gram-negative bacteria as well as anaerobes.

2.2.2. Antimycobacterial activity

2.2.2.1. Determination of MICs. The newly synthesized compounds were *in vitro* evaluated for their antimycobacterial activity against the *M. tuberculosis* H37Rv strain using the microplate Alamar Blue assay (MABA) method. The MIC values in (μg and μM) are listed in Table 2 for the compounds **3a**, **3b** and **5a–5q** along with isoniazid, rifampicin, and ethambutol as standard drugs for comparison. Among the screened compounds, compounds **3a**, **3b**, **5b** and **5e** have shown *in vitro* inhibitory potency against Mtb with MICs ranging from 4.47 to 66.44 μM. The MIC of NTZ is 20.34 μM and that of TIZ is 11.78 μM. Introducing an azido group to TIZ afforded compound **3a** with improved potency (MIC 10.20 μM), that is, 2-fold more potent. Furthermore, acetylation of compound **3a** provided compound **3b** with an MIC of 4.47 μM that is 5-fold more potent than the parent drug NTZ and 1.7-fold more potent than the standard antitubercular drug ethambutol (MIC = 7.63 μM). Except for **5b** and **5e** with MICs of 66.44 and 59.18 μM, respectively, the conversion of 4-azido **3a** into 1,4-disubstituted 1,2,3-triazoles (**5a–5q**) provided compounds with reduced antimycobacterial activity (Table 2). The lower activity of the triazole derivatives could be accounted for structural rigidity, molecular mass and/or steric effect. Accordingly, 4-azidation and/or acetylation of OH increase the antimycobacterial activity of NTZ, while the introduction of 1,2,3-triazoles is detrimental to the activity.

2.2.2.2. In vitro cytotoxicity. Potential candidates for pre-clinical drug development are typically tested against mammalian cell lines, such as mouse macrophage RAW 264.7 cells, to determine any potential cytotoxic effects the molecule may have on normal human cells. The safety profile of the most potent compounds **3a**, **3b**, **5b** and **5e** was assessed using the 3-(4,5-dimethylthiazol-2-yl)-2,5-diphenyltetrazolium bromide (MTT) assay against mouse macrophage RAW 264.7 cells at 25 μg ml^{-1}. The percentage inhibition is reported in Table 2. The most active compounds are not cytotoxic toward the mouse macrophage RAW 264.7 cells. The ratio between *in vitro* cytotoxicity and antimycobacterial activity (MIC in μg

Table 2 The anti-mycobacterial activity of test compounds against *M. tuberculosis* $H_{37}Rv$, cytotoxicity and selectivity index (SI)

Compd No.	MIC[a] against the Mtb $H_{37}Rv$ strain (μg mL^{-1})	MIC against the Mtb $H_{37}Rv$ strain (μM)	Cytotoxicity against mouse macrophage RAW 264.7 (% inhibition)	Selectivity index
3a	3.125	10.20	28.53	8
3b	1.56	4.47	17.54	16
5a	>25	—		
5b	25	66.44	27.5	1
5c	>25	—	—	—
5d	>25	—	—	—
5e	25	59.18	27.60	1
5f	>25	—	—	—
5g	>25	—	—	—
5h	>25	—	—	—
5i	>25	—	—	—
5j	>25	—	—	—
5k	>25	—	—	—
5l	>25	—	—	—
5m	>25	—	—	—
5n	>25	—	—	—
5o	>25	—	—	—
5p	>25	—	—	—
5q	>25	—	—	—
NTZ	6.25	20.34	20.65	4
TIZ	3.12	11.78	—	—
Isoniazid	0.05	0.36	—	—
Rifampicin	0.1	0.12		
Ethambutol	1.56	7.63		

[a] Values are means of three experiments.

ml^{-1}) determines the selectivity index (SI). The most promising antimycobacterial compounds **3a** and **3b** exhibited selectivity indices >8 and 16, respectively, revealing higher safety margins than the parent drugs NTZ and TIZ.

2.2.3. Structure–activity relationships. Results from antibacterial and antimycobacterial testing revealed that structural modifications significantly affected the pattern of activity. For example, 4-azidation (**3a**) and/or acetylation of the OH group of the salicylyl moiety (**3b**) improved both activities in comparison with NTZ. Moreover, introducing a triazole ring at the fourth position of the salicylyl moiety greatly improved the antibacterial activity and afforded compounds (**5f**, **5j**, **5n** and **5o**) more potent than the reference drugs (NTZ and ciprofloxacin), while it was detrimental to the antimycobacterial activity. Furthermore, the nature of the substituent at the fourth position of the triazole ring significantly affected the activity where relatively large lipophilic groups such as 5-haloisatins (**5l**, **5m**, **5n**), 5-methylisatin (**5o**), benzothiazole (**5q**) and phenylpiperazine (**5j**) showed the highest broad-spectrum activity, while small hydrophilic groups such as CH_2OH (**5a**) or CH_2COOH (**5b**) showed much lower activity against all strains.

2.3. Molecular docking

2.3.1. Docking with bacterial targets. For exploring the possible mechanism by which the new NTZ derivatives affect their microbial targets, a molecular docking study was performed within crystal structures of three common microbial proteins, pyruvate ferredoxin oxidoreductase (PFOR), glucosamine-6-phosphate synthase (G6PS) and Mtb dihydrofolate reductase (DHFR), and the binding affinity (*S* score in kcal mol^{-1}) is listed in Table 3. The designed compounds are multifunctional and are proposed to be multitarget antimicrobial agents acting on different bacterial protein targets such as PFOR, G6PS and DHFR. The high binding scores against PFOR indicate that it is the main target of the compounds. This conclusion is supported by the activity of the compounds against anaerobes. Moreover, the high binding score against G6PS and to a lesser extent against DHFR and the high activity against aerobes mean that the compounds could affect other targets such as G6PS and DHFR.

These target proteins are known for their involvement in the biochemical pathways regarding their respective biological functions. It has been elucidated that NTZ is

Table 3 Binding affinity of the most active compounds to three bacterial proteins: pyruvate ferredoxin oxidoreductase (PFOR), glucosamine-6-phosphate synthase (G6PS) and Mtb dihydrofolate reductase (DHFR)

PFOR		G6PS		DHFR	
Compd No.	*S* score (kcal mol^{-1})	Compd No.	*S* score (kcal mol^{-1})	Compd No.	*S* score (kcal mol^{-1})
NTZ	−7.39	NTZ	−7.06	NTZ	−6.14
5c	−8.72	**3a**	−7.10	**3a**	−6.35
5e	−8.64	**3b**	−7.23	**3b**	−6.68
5f	−8.87	**5c**	−7.48	**5b**	−6.65
5m	−7.78	**5n**	−7.99	**5e**	−7.43
5n	−8.05	**5o**	−8.15		
5o	−8.37	**5q**	−8.49		

active as an amidic anion which outcompetes the substrate pyruvate by targeting thiamine pyrophosphate (TPP) that is a cofactor of pyruvate ferredoxin oxidoreductase, which ultimately blocks the production of acetyl-CoA and CO_2, necessary for anaerobic energy metabolism.[37,38] Thus, *in silico* docking simulations of the most active compounds **5c**, **5e**, **5f**, **5m**, **5n** and **5o** against *H. pylori* (PFOR utilizing microorganism) were employed. The docking protocol was validated by redocking the co-crystallized ligand pyruvate into the active site of PFOR which was found to have a binding affinity (*S* score) of −4.45 kcal mol^{-1} with an RMSD of 0.2282 Å, and the results were compared with the co-crystallized ligand and the parent NTZ. Interestingly, compounds **5c**, **5e**, **5f**, **5m**, **5n** and **5o** showed high docking scores (*S* = −7.39 to −8.89 kcal mol^{-1}) along with better orientation within the active site of PFOR comparable to their parent NTZ (*S* = −7.39 kcal mol^{-1}) as shown in Fig. 3, S48–S54 and Table S2.† Additionally, visual inspection of interactions was found with the key amino acid residues Thr31, Arg114, and Asp996 which are mainly mediated by H-bonds with an average length of 3.23, 3.04 and 3.06 Å, respectively.

Furthermore, glucose-6-phosphate synthase catalyzes the initial step in a pathway that results in the production of uridine 5′-diphospho-*N*-acetyl-D-glucosamine (UDP-GlcNAc), a crucial structural component of the bacterial peptidoglycan, the lipopolysaccharide of Gram-negative bacteria, chitin, and the mannoproteins found in fungal cell walls.[71,72] Recently, G6PS was the focus of *in silico* investigation using substituted thiazoles that demonstrated a strong binding affinity for this enzyme.[43,72] Validation of the docking study was carried out by redocking of co-crystallized ligand glucose-6-phosphate G6P in its active site which was found to have an *S* score of −6.22 with an RMSD of 0.4788 Å. The prospective docking of the most active NTZ derivatives (as anions) **3b**, **5c**, **5j**, **5n**, **5o** and **5q** along with NTZ within the active site of G6PS could give a good idea about their mode of inhibition. Obviously, all test compounds depicted strong and well-adapted interaction (−7.06 to −8.15 kcal mol^{-1}) with G6PS in its active site (Ser 347, Ser 349 and Thr 352) which was primarily driven by H-bonds with an average length of 2.89, 3.23, and 2.85 Å, respectively, where the most active compounds had greater binding affinity and better interaction than the parent NTZ (Fig. 4, S55–S61 and Table S3†).

It is important to note that the H-bonding with the ionized nitro group and amide functional group in addition to extra-binding interactions of 1,2,3-triazole and 1,2,3-triazole coupled moieties was primarily responsible for the higher binding affinity and improved interaction of the active compounds comparable with their parent NTZ to the active sites of both PFOR and G6PS which support the enhanced antibacterial activity of the synthesized derivatives against the tested bacterial strains.

On the other hand, dihydrofolate reductase (DHFR) is an essential enzyme for the *de novo* synthesis of methionine, purines, and deoxythymidine monophosphate (dTMP) of mycobacteria.[73,74] Moreover, the bioactive metabolite of 4-ASA was described to inhibit Mtb DHFR and interrupt Mtb folate metabolism.[75,76] Thus, *in silico* docking simulations were performed within the DHFR protein in order to explore the mechanism of action of such a class of compounds. Apparently, compounds **3a**, **3b**, **5b** and **5e** suited the DHFR active site well and had a relatively good binding affinity (−6.65 to −7.43 kcal mol^{-1}) comparable to the co-crystallized ligand (Fig. 5, S62–S66 and Table S4†). Commonly, all the test compounds primarily interacted with

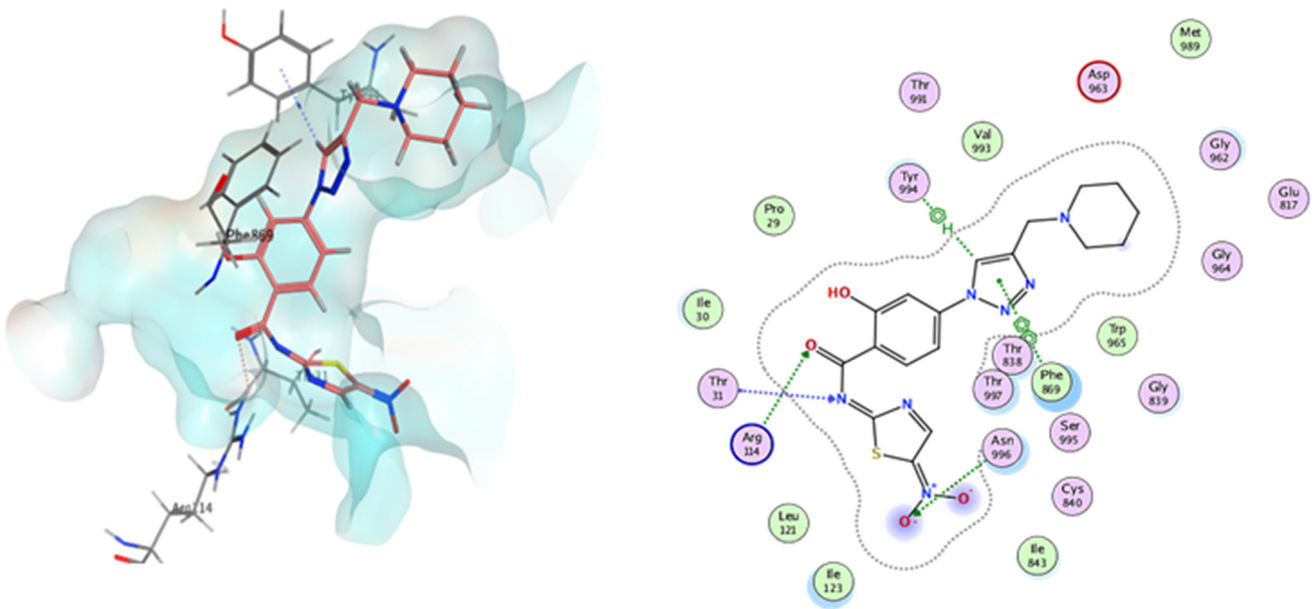

Fig. 3 Ligand interactions: 2D and 3D diagrams of compound **5f** within the active site of the *H. pylori* PFOR enzyme protein crystal structure (PDB ID: 2C42).

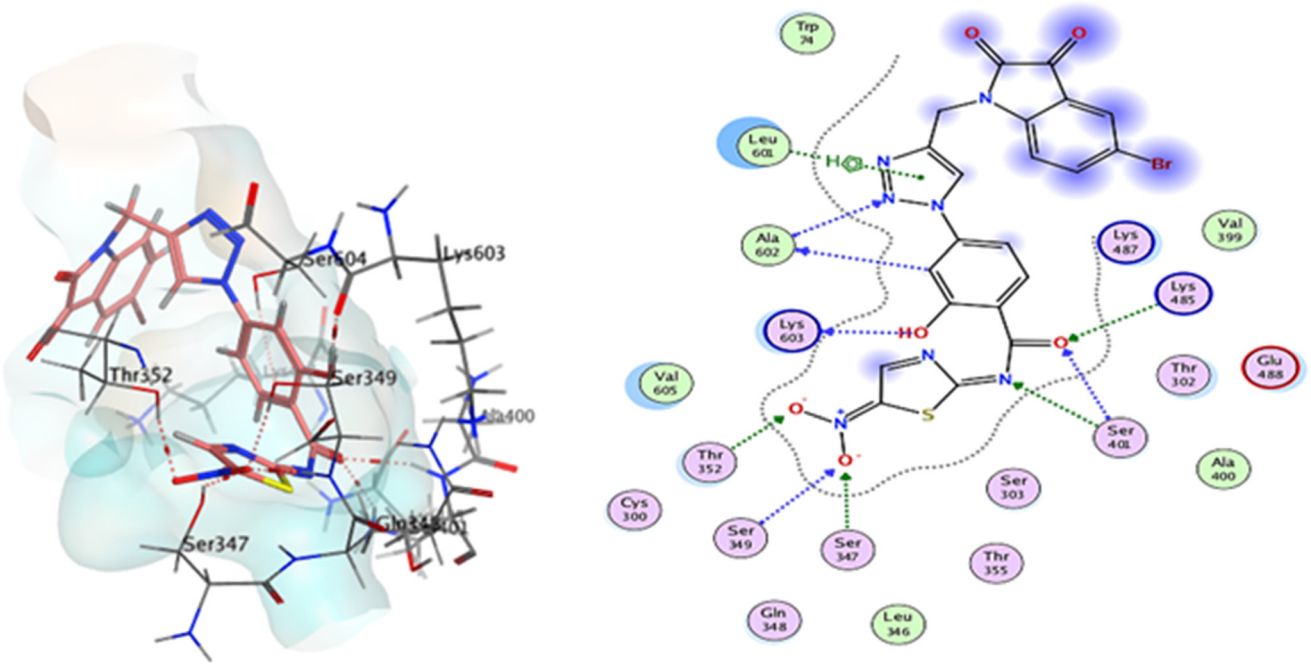

Fig. 4 Ligand interactions: 2D and 3D diagrams of compound **5n** within the active site of the glucosamine-6-phosphate synthase (G6PS) protein crystal structure (PDB ID: 2J6H).

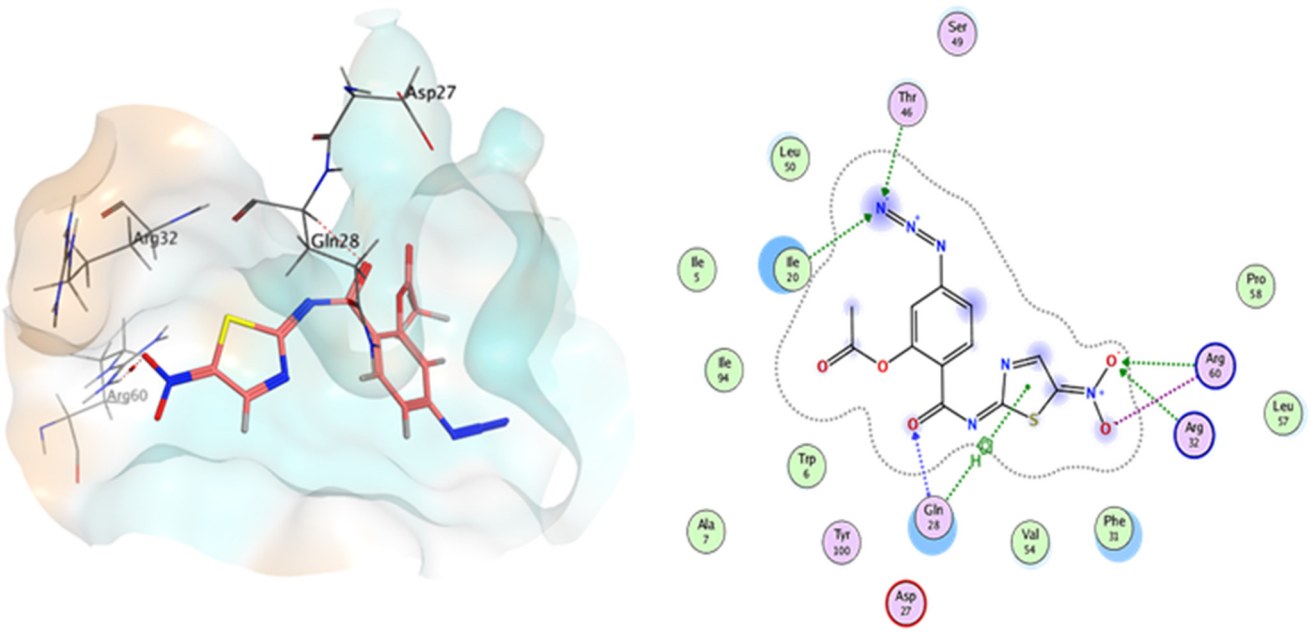

Fig. 5 Ligand interactions: 2D and 3D diagrams of compound **3b** within the active site of the dihydrofolate reductase (DHFR) protein crystal structure (PDB ID: 6DDW).

the key amino acids lining the active site *via* H-bonding with Arg60, with an average bond length of 3.19 Å, and additional ionic interaction with Arg32, which is a known interaction essential for inhibition of catalytic activity of DHFR and could be utilized to explain why such a class of compounds could be possible anti-microbial candidates with anti-Mtb activity.

The higher binding affinity and improved interaction of the new compounds with the active sites of PFOR, G6PS and DHFR in comparison with their parent NTZ found through docking simulations could be attributed to the extra-binding interactions of the 1,2,3-triazole ring and appended moiety with the key amino acids lining the active sites. Thus, the docking studies revealed that the new compounds interact

with the three targets which increase the possibility of multitarget opportunity.

2.4. *In silico* prediction of drug-likeness

The physicochemical characteristics of molecules are influenced by a combination of intricate structural properties, determining their similarity to established drugs. Within this context, hydrophobicity, molecular size, and flexibility stand as pivotal physicochemical traits influencing the behavior of molecules in living organisms.[77] Hence, an assessment was conducted to ascertain the adherence of recently synthesized compounds to Lipinski's rule of five, which evaluates factors like molecular weight, count of hydrogen-bond donors and acceptors, and the logarithmic octanol/water partition coefficient ($\log P$ (O/W)).[78] This calculation aimed to discern how the modifications made to the nitazoxanide structure impacted its physicochemical characteristics. The newly synthesised compounds' molecular properties were calculated using the SwissADME website[79] and are listed in Table 4. Research indicates that for a compound to be reasonably absorbed, its $\log P$ value should ideally fall between −0.4 and 5.[80] In accordance with this criterion, all tested compounds displayed $\log P$ values ranging from 0.22 to 2.99, aligning with acceptable ranges and predicting favorable oral absorption. As per Lipinski's rule of five, a compound is likely to be orally active if it doesn't violate more than one of the specified criteria.[81] Consequently, it's noteworthy that all analyzed compounds adhered to Lipinski's rule, implying their potential as orally active substances.

3. Conclusion

A series of nineteen new and multifunctional derivatives of NTZ appended with common antimicrobial pharmacophores through the 1,2,3-triazole ring were synthesized, characterized, and evaluated for their antibacterial and antimycobacterial activities. Most of the compounds showed much higher potency and broad-spectrum activities compared to the parent drug NTZ against all the screened strains, particularly, compounds **5f**, **5j**, **5n** and **5o** with MICs of 0.87–9.00 μM. Some compounds are more potent than or equipotent to the standard drug ciprofloxacin. Moreover, compounds **3a** and **3b** revealed good antimycobacterial activity with MIC values of 10.20 and 4.47 μM and were 2- and 5-fold more potent than the parent NTZ with higher safety margins. The results reveal that azidation and/or acetylation of NTZ improve its antibacterial and antimycobacterial activities. Introducing a 1,2,3-triazole ring at the 4-position of NTZ greatly improved the antibacterial activity, while it was detrimental to the antimycobacterial activity. Docking simulation studies were employed for the most active antimicrobial compounds against some protein targets to explore their possible mechanisms of action including PFOR, G6PS and DHFR. The result of these studies showed that the active compounds could interact actively with the respective microbial proteins. The predicted ADME properties were found to be in the acceptable ranges.

Table 4 Calculated physicochemical properties of the designed compounds (**3a–b**, **5a–q**)

Compd No.	MWt	HBD	HBA	Log P (O/W)	Lip. violation
3a	306.26	2	8	1.01	0
3b	348.29	1	9	1.29	0
5a	362.32	3	8	0.16	0
5b	376.30	3	9	0.22	0
5c	390.33	2	9	0.74	0
5d	408.39	2	7	1.99	0
5e	422.42	2	7	2.29	0
5f	429.45	2	8	1.41	0
5g	415.43	2	8	1.06	0
5h	431.43	2	9	0.75	0
5i	444.47	2	9	0.42	0
5j	506.54	2	8	1.70	1
5k	491.44	2	9	1.02	0
5l	509.43	2	10	1.38	1
5m	525.88	2	9	1.61	1
5n	570.33	2	9	1.69	1
5o	505.46	2	9	1.3	1
5p	521.46	2	10	1.00	1
5q	511.56	2	8	2.99	1

4. Experimental

4.1. Chemistry

All solvents and reagents were obtained from commercial suppliers and used without purification except for tetrahydrofuran which was dried by reflux with sodium metal and benzophenone followed by distillation. Melting points were determined using an electrothermal melting point apparatus [Stuart Scientific, model SMP3, UK] and were uncorrected. Pre-coated silica gel plates (Kieselgel 0.25 mm, 60G F_{254}, Merck, Germany) were used for TLC monitoring of the chemical reactions. Ethyl acetate/hexane (3 : 1 v/v) was used as a developing solvent system, unless otherwise specified and the visualization of the spots was detected by using an ultraviolet lamp Spectroline, model CM-10, USA at a wavelength λ = 254 nm. IR spectra (KBr discs) were recorded on Thermo Scientific Nicolet IS10 FT IR spectrometers (Thermo Fischer Scientific, USA) at the Faculty of Science, Assiut University, Assiut, Egypt. ^{1}H-NMR (400 MHz) and ^{13}C-NMR (100 MHz) spectra were scanned on an Avance-III, high-performance FT-NMR spectrometer (Bruker, BioSpin International AG-Switzerland) at the Faculty of Science, Zagazig University, Al Sharqia, Egypt. Chemical shifts are expressed in δ-values (ppm) relative to TMS as an internal standard, using DMSO-d_6 as a solvent. Coupling constants (J) are reported in Hertz (Hz). ESI-MS spectra were determined using an Advion compact mass spectrometer (CMS) NY|USA equipped with an electrospray ionization (ESI) interface at the labs of Nawah-Scientific, El Mokattam, Cairo, Egypt. Elemental microanalyses were performed on an elemental analyzer model FLASH 2000 Thermo Fisher at the Regional Center for Mycology and

Biotechnology (RCMB), Faculty of Science, Al-Azhar University, Nasr City, Cairo, Egypt for all new compounds.

4.1.1. Synthesis of 4-azido-salicylic acid (2). The synthesis was achieved according to reported procedures.[63] 4-ASA (5.0 g, 33 mmol) was dissolved in a solution of H_2SO_4 (25 mL) and H_2O (130 mL) in a 1 L beaker. The resulting mixture was cooled to 0 °C, whereupon the amine was diazotized with a solution of $NaNO_2$ (2.8 g, 40 mmol) in H_2O (25 mL). After stirring for 1 h at 0 °C, a solution of NaN_3 (3.6 g, 56 mmol) in H_2O (20 mL) was added dropwise to the chilled reaction. The suspension was kept in an ice-bath and stirred for 1 h and was then allowed to stand overnight at room temperature. The product was filtered from H_2O and recrystallized from EtOH/H_2O to obtain compound **2** as brown crystals. Yield: (5.1 g, 87%); m.p.: 198–200 °C.

4.1.2. 4-Azido-2-hydroxy-*N*-(5-nitro-1,3-thiazol-2-yl) benzamide (3a). To a solution of compound **2** (2 g, 11 mmol, 1 equivalent) in dry THF (10 ml) in a 50 ml round-bottom flask was added *N*,*N*′-carbonyldiimidazole (2.2 g, 13 mmol, 1.2 equivalent), and the resulting mixture was heated under reflux for 3 h. The reaction was allowed to cool to room temperature and then 2-amino-5-nitrothiazole (1.6 g, 11 mmol, 1 equivalent) was added and reflux was continued for 6 h. After completion of the reaction, THF was evaporated, and the produced solid was treated with a saturated $NaHCO_3$ solution and stirred for ¼ h. The crude product was filtered, washed with water and recrystallized from DMF/water. Yield: 77%; m.p.: 189–190 °C; IR (υ cm^{-1}, KBr): 3455 (phenolic O–H), 3214 (N–H), 3101 (Ar–H) 2121 (–N═N═N), 1666 (C═O); ^{1}H-NMR (δ ppm): δ 6.51–6.59 (m, 2H, Ar–H), 7.92 (d, J = 8.1 Hz, 1H), 8.51 (s, N–H), 8.97 (s, 1H, thiazole–H), 14.22 (s, 1H, OH); ^{13}C-NMR (δ ppm): 106.91, 110.73, 114.07, 116.41, 132.37, 142.82, 145.60, 159.47, 163.30, 166.03; ESI-MS (*m*/*z*): calcd. $[M–H]^-$ for $C_{10}H_5N_6O_4S$ 305.0, found: 305.3; elemental microanalysis % for $C_{10}H_6N_6O_4S$: calculated/found: 39.22/39.49 (%C), 1.97/2.15 (%H), 27.44/27.68 (%N) and 10.47/10.50 (%S).

4.1.3. 5-Azido-2-[(5-nitrothiazol-2-yl)carbamoyl]phenyl acetate (3b). A mixture of compound **3a** (0.1 g, 0.33 mmol), acetic anhydride (2 mL) and 2 drops of conc. H_2SO_4 was stirred at 60 °C for 1 hour. After that, the mixture was allowed to cool to room temperature and cold H_2O (5 mL) was added and then the obtained precipitate was filtered, washed with cold H_2O and dried. Yield: 71%; m.p.: 185–186 °C; IR (υ cm^{-1}, KBr): 3272 (N–H), 3109 (Ar–H), 2929 (aliphatic C–H), 2117 (–N═N═N), 1765 (ester C═O), 1655 (amidic C═O); ^{1}H-NMR (δ ppm): 2.25 (s, 3H, $–CH_3$), 7.12–7.21 (m, 2H, Ar–H), 7.90 (d, J = 8.5 Hz, 1H, Ar–H), 8.68 (s, 1H, thiazole–H); ^{13}C-NMR (δ ppm): 21.21, 107.00, 111.19, 113.55, 116.73, 132.72, 142.61, 146.15, 159.02, 162.06, 165.10, 172.36; elemental microanalysis % for $C_{12}H_8N_6O_5S$: calculated/found: 41.38/41.59 (%C), 2.32/2.47 (%H), 24.13/24.41 (%N) and 9.21/9.45 (%S).

4.1.4. Synthesis of propargylated derivatives (4f–q)[64–70]

*4.1.4.1. Synthesis of propargylated piperidine (**4f**).*[64] To a solution of piperidine (2 mL, 20 mmol, 2.5 equivalent) in DCM (4 mL) was added dropwise propargyl bromide (80% wt in toluene, 1 mL, 8 mmol, 1 equivalent), and the resulting mixture was allowed to stir at room temperature for 15 h. DCM was evaporated and the residue was extracted with 10 mL diethyl ether, washed with H_2O, dried over Na_2SO_4 for 4 h to afford the target as an orange oil after evaporation of the solvent and was used directly in the click step without further purification.

*4.1.4.2. Synthesis of propargylated pyrrolidine (**4g**) and morpholine (**4h**).*[65] A solution of amine (2 mL, 23.30 mmol, 2 equivalent) and diethyl ether (4 mL) was cooled to 0 °C. Propargyl bromide (80% wt in toluene, 1.7 mL, 11.5 mmol, 1 equivalent) was added to the solution dropwise, and after 5 minutes, the reaction was brought to room temperature and stirring was continued for 12 h. The precipitated solid was discarded and the filtrate was diluted with H_2O, extracted three times with EtOAc, washed with brine, dried over Na_2SO_4, filtered, and concentrated under vacuum to obtain the desired products as yellow oils that were used directly without further purification.

*4.1.4.3. Synthesis of propargylated piperazine derivatives (**4i** and **j**).*[66] To a mixture of appropriate piperazine (6.73 mmol, 1 equivalent) and K_2CO_3 (1.86 g, 13.46 mmol, 2 equivalent) in dry THF (10 mL) was added propargyl bromide (80% wt in toluene, 1 mL, 6.73 mmol, 1 equivalent) with stirring at rt for 5 minutes, and then the mixture was brought to reflux for 24 h. After that, the reaction mixture was cooled, filtered and evaporated to obtain the target propargylated derivatives (**4i** and **4j**) as orange oils that were used directly without further purification.

*4.1.4.4. Synthesis of propargylated un/5-substituted isatins (**4k–p**).*[67–69] To a solution of 5-(un)substituted isatin (3.36 mmol, 1 equivalent) in DMF (3 mL) was added K_2CO_3 (1.39 g, 10.08 mmol, 3 equivalent) and the mixture was stirred for ¼ h, then propargyl bromide (80% wt in toluene, 0.6 mL, 4.04 mmol, 1.2 equivalent) was added and the reaction mixture was stirred at room temperature for 3 h. Upon addition of H_2O (15 mL), the propargylated isatins were precipitated, filtered, washed with H_2O and recrystallized from EtOH/H_2O and air dried (% yield and melting points are listed in Table 5).

*4.1.4.5. Synthesis of propargylated 2-mercaptobenzothiazole (**4q**).*[70] To a solution of 2-mercaptobenzothiazole (0.56 g, 3.36

Table 5 Propargylated isatins: yield and melting point (**4k–p**)

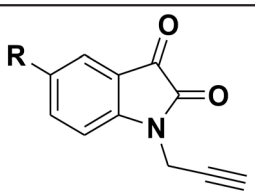

(4b-g)

Compd No.	R	Yield (%)	m.p. (°C)
4k	H	84	158–160
4l	F	81	148–152
4m	Cl	79	168–170
4n	Br	85	160–162
4o	CH_3	76	156–159
4p	OCH_3	83	133–134

mmol, 1 equivalent) in DMF (3 mL) was added K_2CO_3 (0.5 g, 3.36 mmol, 1 equivalent) and the mixture was stirred for ¼ h, then propargyl bromide (80% wt in toluene, 0.5 mL, 3.36 mmol, 1 equivalent) was added and the reaction mixture was stirred at room temperature for 2 h. H_2O (15 mL) was added. The product was filtered, washed with H_2O and recrystallized from EtOH to afford **4q** as white crystals in a 90% yield with m.p.: 82–84 °C (as reported).

4.1.5. Synthesis of sodium ascorbate.[82] To a solution of ascorbic acid (4.4 g) in H_2O (4 mL) was added $NaHCO_3$ (2.1 g) and the solution was stirred at room temperature for 1 h. After that, anhydrous isopropanol (20 mL) was added, and stirring was continued for an additional 1 h. The precipitated sodium ascorbate was allowed to settle down, and the supernatant was poured off, and additional isopropanol (20 mL) was added; the mixture was thoroughly stirred, and the formed sodium ascorbate was filtered, washed with isopropanol (10 mL) and dried over $CaCl_2$ in a light-opaque desiccator.

4.1.6. General method for synthesis of 1,2,3-triazoles (5a–q). To a 25 mL round-bottom flask were added compound **3a** (0.1 g, 327 μmol), appropriate alkyne/propargylated compound (**4a–q**) (327 μmol), $CuSO_4{\cdot}5H_2O$ (0.016 g, 66 μmol) and freshly prepared sodium ascorbate (0.064 g, 327 μmol) dissolved in 1 : 1 THF/H_2O (5 mL), and the resulting mixture was stirred for 2–4 h at rt. The progress of the reaction was monitored by TLC and after the reaction completion, THF was evaporated, and H_2O (5 mL) was added. The crude product was collected by suction filtration, washed with H_2O and recrystallized from DMF/H_2O.

*4.1.6.1. 2-Hydroxy-4-[4-(hydroxymethyl)-1H-1,2,3-triazol-1-yl]-N-(5-nitrothiazol-2-yl)benzamide (**5a**).* Reaction time: 4 h; yield: (0.1 g, 76%); m.p.: 154 °C (charring); ^{1}H-NMR (δ ppm): 4.27 (br.s, 1H, O–H), 4.62 (s, 2H, –CH_2), 7.52–7.59 (m, 2H, Ar–H), 8.01 (s, 1H, triazole–H), 8.15 (d, J = 8.3 Hz, 1H, Ar–H), 8.78 (s, 1H, thiazole–H), 8.96 (s, 1H, N–H), 12.06 (br.s, 1H, O–H); ESI-MS: m/z calculated for $C_{13}H_9N_6O_5S$ $[M–H]^-$: 361.0, found: 361.3; elemental microanalysis % for $C_{13}H_{10}N_6O_5S$: calculated/found: 43.09/43.23 (%C), 2.78/3.01 (%H), 23.19/23.45 (%N) 8.85/8.97 (%S).

*4.1.6.2. 1-[3-Hydroxy-4-(5-nitrothiazol-2-ylcarbamoyl)phenyl]-1H-1,2,3-triazole-4-carboxylic acid (**5b**).* Reaction time: 3 h; yield: (0.1 g, 82%); m.p.: 260 °C (charring); IR (υ cm^{-1}, KBr): 3500–2500 (carboxylic O–H), 3400 (O–H) 3250 (N–H), 3094 (Ar–H), 1708 (carboxylic C=O), 1663 (amidic C=O); ^{1}H-NMR (δ ppm): 7.55–7.61 (m, 2H, Ar–H), 8.04 (d, J = 8.5 Hz, 1H, Ar–H), 8.73 (s, 1H, triazole–H), 8.92 (s, 1H, N–H), 9.47 (s, 1H, thiazole–H), 13.73 (s, 1H, –COOH), 14.34 (s, 1H, O–H); elemental microanalysis % for $C_{13}H_8N_6O_6S$: calculated/found: 41.49/41.75 (%C), 2.14/2.27 (%H), 22.33/22.59 (%N) 8.52/8.43 (%S).

*4.1.6.3. Methyl-1-[3-hydroxy-4-(5-nitrothiazol-2-ylcarbamoyl) phenyl]-1H-1,2,3-triazole-4-carboxylate (**5c**).* Reaction time: 3 h; yield: (0.1 g, 79%); m.p.: 257–259 °C (charring); IR (υ cm^{-1}, KBr): 3435 (O–H), 3264 (N–H), 3161 (Ar–H), 2957 (C–H, aliphatic), 1738 (ester C=O), 1661 (amidic C=O); ^{1}H-NMR (δ ppm): 3.90 (s, 3H, –CH_3), 7.56–7.61 (m, 2H, Ar–H), 7.04–8.10 (m, 2H, Ar–H and triazole–H), 8.93 (s, 1H, N–H), 9.59 (s, 1H, thiazole–H), 13.38 (br.s, 1H, O–H); ESI-MS: m/z calculated for $C_{14}H_9N_6O_6S$ $[M–H]^-$: 389.0, found: 389.3; elemental microanalysis % for $C_{14}H_{10}N_6O_6S$: calculated/found: 43.08/43.21 (%C), 2.58/2.69 (%H), 21.53/21.70 (%N) 8.21/8.30 (%S).

*4.1.6.4. 2-Hydroxy-N-(5-nitrothiazol-2-yl)-4-(4-phenyl-1H-1,2,3-triazol-1-yl)benzamide (**5d**).* Reaction time: 2.5 h; yield: (0.11 g, 83%); m.p.: 276–278 °C (charring); ^{1}H-NMR (δ ppm): 7.09–7.81 (m, 7H, Ar–H), 7.96 (d, J = 7.4 Hz, 1H, Ar–H), 8.13 (s, 1H, triazole–H), 8.80 (s, 1H, N–H), 9.38 (s, 1H, thiazole), 11.66 (br.s, 1H, O–H); ^{13}C-NMR (δ ppm): 108.26, 109.48, 119.54, 120.04, 125.84, 125.87, 128.79, 129.51, 130.63, 131.82, 140.20, 145.55, 147.82, 156.47, 162.32, 170.49; ESI-MS: m/z calculated for $C_{18}H_{11}N_6O_4S$ $[M–H]^-$: 407.0, found: 407.3; elemental microanalysis % for $C_{18}H_{12}N_6O_4S$: calculated/found: 52.94/53.15 (%C), 2.96/3.04 (%H), 20.58/20.79 (%N) 7.85/7.96 (%S).

*4.1.6.5. 2-Hydroxy-N-(5-nitrothiazol-2-yl)-4-(p-tolyl-1H-1,2,3-triazol-1-yl)benzamide (**5e**).* Reaction time: 4 h; yield: (0.12 g, 87%); m.p.: 278–280 °C (charring); ^{1}H-NMR (δ ppm): 2.36 (s, 3H, –CH_3), 7.32 (d, J = 7.7 Hz, 2H, Ar–H), 7.55–7.63 (m, 2H, Ar–H), 7.85 (d, J = 7.6 Hz, 2H, Ar–H), 8.06–8.14 (m, 2H, Ar–H and triazole–H), 8.57 (s, 1H, N–H), 9.34 (s, 1H, thiazole–H), 12.21 (br.s, 1H, O–H); elemental microanalysis % for $C_{19}H_{14}N_6O_4S$: calculated/found: 54.02/54.29 (%C), 3.34/3.47 (%H), 19.90/20.04 (%N) 7.59/7.68 (%S).

*4.1.6.6. 2-Hydroxy-N-(5-nitrothiazol-2-yl)-4-{4-[(piperidin-1-yl) methyl]-1H-1,2,3-triazol-1-yl}benzamide (**5f**).* Reaction time: 2 h; yield: (0.11 g, 79%); m.p.: 228 °C (charring); ^{1}H-NMR (δ ppm): 1.48–1.91 (m, 6H, –$(CH_2)_3$ of piperidinyl), 2.94–3.07 (m, 4H, N$(CH_2)_2$ of piperidinyl), 4.20 (s, 2H, –CH_2), 7.39–7.43 (m, 2H, Ar–H), 8.08–8.10 (m, 2H, Ar–H and triazole–H), 8.61 (s, 1H, N–H), 8.92 (s, 1H, thiazole–H), 15.60 (br.s, 1H, O–H); ^{13}C-NMR (δ ppm): 22.30, 23.86, 52.83, 59.18, 108.58, 109.54, 119.87, 124.79, 131.74, 135.04, 139.99, 145.89, 150.05, 154.64, 162.62, 170.86; elemental microanalysis % for $C_{18}H_{19}N_7O_4S$ (429.45): calculated/found: 50.34/50.60 (%C), 4.46/4.52 (%H), 22.83/22.95 (%N) 7.47/7.42 (%S).

*4.1.6.7. 2-Hydroxy-N-(5-nitrothiazol-2-yl)-4-{4-[(pyrrolidin-1-yl)methyl]-1H-1,2,3-triazol-1-yl}benzamide (**5g**).* Reaction time: 2 h; yield: (0.11 g, 81%); m.p.: 264 °C (charring); ^{1}H-NMR (δ ppm): 1.94–1.98 (m, 4H, –$(CH_2)_2$ of pyrrolidinyl), 3.33 (s, 4H, –N–$(CH_2)_2$ of pyrrolidinyl), 4.58 (s, 2H, –CH_2), 7.39–7.49 (m, 2H, Ar–H), 7.95 (s, 1H, triazole–H), 8.11 (d, J = 8.39 Hz, 1H, Ar–H), 8.64 (s, 1H, N–H), 9.00 (s, 1H, thiazole–H), 10.12 (br.s, 1H, O–H); elemental microanalysis % for $C_{17}H_{17}N_7O_4S$: calculated/found: 49.15/49.33 (%C), 4.12/4.29 (%H), 23.60/23.76 (%N) 7.72/7.94 (%S).

*4.1.6.8. 2-Hydroxy-4-{4-[(morpholin-4-yl)methyl]-1H-1,2,3-triazol-1-yl}-N-(5-nitrothiazol-2-yl)benzamide (**5h**).* Reaction time: 3 h; yield: (0.11 g, 78%); m.p.: 204 °C (charring); ^{1}H-NMR (δ ppm): 2.98–3.22 (m, 4H, N$(CH_2)_2$ of morpholinyl), 3.86–3.90 (m, 4H, O$(CH_2)_2$ of morpholinyl), 4.55 (s, 2H, –CH_2), 7.45–7.54 (m, 2H, Ar–H), 8.10 (d, J = 8.5 Hz, 1H, Ar–H), 8.63 (s, 1H, triazole–H), 8.74 (s, 1H, N–H), 9.01 (s, 1H, thiazole–H), 13.58 (br.s, 1H, O–H); ^{13}C-NMR (δ ppm): 49.91, 50.78, 63.30, 108.20,

110.11, 118.47, 125.44, 131.94, 137.38, 139.82, 139.83, 143.50, 160.18, 165.93, 167.57; ESI-MS: *m*/*z* calculated for $C_{17}H_{16}N_7O_5S$ $[M-H]^-$: 430.0, found: 430.3; elemental microanalysis % for $C_{17}H_{17}N_7O_5S$: calculated/found: 47.33/47.60 (%C), 3.97/4.15 (%H), 22.73/22.94 (%N) and 7.43/7.28 (%S).

*4.1.6.9. 2-Hydroxy-4-{4-[(4-methylpiperazin-1-yl)methyl]-1H-1,2,3-triazol-1-yl}-N-(5-nitrothiazol-2-yl)benzamide (**5i**).* Reaction time: 3 h; yield: (0.12 g, 83%); m.p.: 175–177 °C (charring); ^{1}H-NMR (δ ppm): 2.50–2.82 (m, 11H, $N(CH_2)_4$ of piperazinyl and $-CH_3$), 3.71 (s, 2H, $-CH_2$), 7.36–7.40 (m, 2H, Ar–H), 8.06–8.08 (m, 2H, Ar–H and triazole–H), 8.53 (s, 1H, N–H), 8.78 (s, 1H, thiazole–H), 15.57 (br.s, 1H, O–H); elemental microanalysis % for $C_{18}H_{20}N_8O_4S$: calculated/found: 48.64/48.91 (%C), 4.54/4.68 (%H), 25.21/25.47 (%N) and 7.21/7.09 (%S).

*4.1.6.10. 2-Hydroxy-N-(5-nitrothiazol-2-yl)-4-{4-[(4-phenylpiperazin-1-yl)methyl]-1H-1,2,3-triazol-1-yl}benzamide (**5j**).* Reaction time: 2 h; yield: (0.13 g, 79%); m.p.: 271–273 °C (charring); ^{1}H-NMR (δ ppm): 3.12–3.56 (m, 4H, $N(CH_2)_2$ of piperazinyl), 3.82–3.83 (m, 4H, $N(CH_2)_2$ of piperazinyl), 4.63 (s, 2H, $-CH_2$), 6.85–7.29 (m, 6H, Ar–H), 7.53 (d, J = 8.5, 1H, Ar–H), 7.66 (s, 1H, triazole–H), 8.11 (d, J = 8.4, 1H, Ar–H), 8.74 (s, 1H, N–H), 9.07 (s, 1H, thiazole–H), 11.22 (br.s, 1H, O–H); ^{13}C-NMR (δ ppm): 45.45, 49.32, 50.38, 108.14, 110.70, 115.98, 117.82, 120.02, 125.58, 126.03, 129.09, 132.31, 137.63, 140.08, 142.46, 149.49, 154.49, 158.89, 165.78; elemental microanalysis % for $C_{23}H_{22}N_8O_4S$: calculated/found: 54.54/54.78 (%C), 4.38/4.50 (%H), 22.12/22.39 (%N) and 6.33/6.41 (%S).

*4.1.6.11. 2-Hydroxy-N-(5-nitrothiazol-2-yl)-4-{4-[(2,3-dioxo-2,3-dihydro-1H-indol-1-yl)methyl]-1H-1,2,3-triazol-1-yl}benzamide (**5k**).* Reaction time: 3 h; yield: (0.14 g, 87%); m.p.: 169 °C (charring); IR (υ cm^{-1}, KBr): 3420 (O–H), 3278 (N–H), 3145 (Ar–H), 2927 (C–H aliphatic), 1734 (isatin ketonic C═O), 1679 (amidic C═O); ^{1}H-NMR (δ ppm): 5.07 (s, 2H, $-CH_2$), 7.13–7.35 (m, 5H, Ar–H), 7.59–7.66 (m, 2H, Ar–H and triazole–H), 8.05 (d, J = 8.1 H, 1H, Ar–H), 8.58 (s, 1H, N–H), 8.92 (s, 1H, thiazole–H), 15.46 (br.s, 1H, O–H); ^{13}C-NMR (δ ppm): 35.11, 107.68, 108.76, 108.94, 111.15, 117.77, 119.25, 121.77, 123.48, 124.52, 131.27, 138.18, 138.19, 139.51, 142.90, 145.31, 150.05, 157.94, 162.13, 170.46, 183.08; ESI-MS: *m*/*z* calculated for $C_{21}H_{12}N_7O_6S$ $[M-H]^-$: 490.0, found: 490.6; elemental microanalysis % for $C_{21}H_{13}N_7O_6S$: calculated/found: 51.32/51.60 (%C), 2.67/2.79 (%H), 19.95/20.19 (%N) and 6.52/6.61 (%S).

*4.1.6.12. 4-{4-[(5-Fluoro-2,3-dioxo-2,3-dihydro-1H-indol-1-yl)methyl]-1H-1,2,3-triazol-1-yl}-2-hydroxy-N-(5-nitrothiazol-2-yl)benzamide (**5l**).* Reaction time: 4 h; yield: (0.13 g, 78%); m.p.: 248 °C (charring); IR (υ cm^{-1}, KBr): 3429 (O–H), 3275 (N–H); 3098 (Ar–H), 2924 (C–H aliphatic), 1736 (isatin ketonic C═O), 1675 (isatin amidic C═O), 1651 (amidic C═O); ^{1}H-NMR (δ ppm): 5.09 (s, 2H, $-CH_2$), 6.95–7.31 (m, 4H, Ar–H), 7.74 (s, 1H, triazole–H), 7.96–8.09 (m, 2H, Ar–H), 8.49 (s, 1H, N–H), 8.94 (s, 1H, thiazole–H), 12.77 (br.s, 1H, O–H); elemental microanalysis % for $C_{21}H_{12}FN_7O_6S$: calculated/found: 49.51/49.78 (%C), 2.37/2.43 (%H), 19.25/19.51 (%N) and 6.29/6.33 (%S).

*4.1.6.13. 4-{4-[(5-Chloro-2,3-dioxo-2,3-dihydro-1H-indol-1-yl)methyl]-1H-1,2,3-triazol-1-yl}-2-hydroxy-N-(5-nitrothiazol-2-yl)benzamide (**5m**).* Reaction time: 4 h; yield: (0.15 g, 88%); m.p.: 252 °C (charring); IR (υ cm^{-1}, KBr): 3429 (O–H), 3262 (N–H), 3146 (Ar–H), 2924 (C–H aliphatic), 1743 (isatin ketonic C═O), 1667 (amidic C═O); ^{1}H-NMR (δ ppm): 5.09 (s, 2H, $-CH_2$), 7.23 (d, J = 8.5 Hz, 1H, Ar–H), 7.39–7.53 (m, 2H, Ar–H), 7.66–7.75 (m, 2H, Ar–H), 8.05 (d, J = 8.6, 1H, Ar–H), 8.70 (d, J = 2.1 Hz, 1H, Ar–H), 8.82 (s, 1H, N–H), 8.92 (s, 1H, thiazole–H), 13.09 (br.s, 1H, O–H); ^{13}C-NMR (δ ppm): 35.59, 105.77, 108.09, 110.79, 113.29, 114.13, 117.90, 122.35, 124.48, 128.15, 132.74, 137.44, 140.81, 142.83, 143.48, 148.96, 158.15, 159.32, 166.31, 166.47, 182.38; elemental microanalysis % for $C_{21}H_{12}ClN_7O_6S$: calculated/found: 47.96/48.15 (%C), 2.30/2.47 (%H), 18.64/18.85 (%N) and 6.10/5.98 (%S).

*4.1.6.14. 4-{4-[(5-Bromo-2,3-dioxo-2,3-dihydro-1H-indol-1-yl)methyl]-1H-1,2,3-triazol-1-yl}-2-hydroxy-N-(5-nitrothiazol-2-yl)benzamide (**5n**).* Reaction time: 4 h; yield: (0.16 g, 89%); m.p.: 275 °C (charring); IR (υ cm^{-1}, KBr): 3435 (O–H), 3250 (N–H), 3145 (Ar–H), 2924 (C–H aliphatic), 1740 (isatin ketonic C═O); ^{1}H-NMR (δ ppm): 5.08 (s, 2H, $-CH_2$), 7.16–7.41 (m, 3H, Ar–H), 7.77–7.83 (m, 2 H, Ar–H), 8.08 (s, 1H, triazole–H), 8.32 (d, J = 2.5 Hz, 1H, Ar–H), 8.82 (s, 1H, N–H), 8.91 (s, 1H, thiazole–H), 14.99 (br.s, 1H, O–H); elemental microanalysis % for $C_{21}H_{12}BrN_7O_6S$: calculated/found: 44.22/44.16 (%C), 2.12/2.63 (%H), 17.19/17.45 (%N) and 5.62/5.49 (%S).

*4.1.6.15. 2-Hydroxy-4-{4-[(5-methyl-2,3-dioxo-2,3-dihydro-1H-indol-1-yl)methyl]-1H-1,2,3-triazol-1-yl}-N-(5-nitrothiazol-2-yl)benzamide (**5o**).* Reaction time: 4 h; yield: (0.13 g, 81%); m.p.: 221 °C (charring); IR (υ cm^{-1}, KBr): 3440 (O–H), 3237 (N–H), 3094 (Ar–H), 2920 (C–H aliphatic), 1735 (isatin ketonic C═O), 1663 (amidic C═O); ^{1}H-NMR (δ ppm): 2.26 (s, 3H, $-CH_3$), 5.04 (s, 2H, $-CH_2$), 7.06–7.13 (m, 2H, Ar–H), 7.40–7.52 (m, 3H, Ar–H), 7.58 (s, 1H, triazole–H), 8.06 (d, J = 8.2 Hz, 1H, Ar–H), 8.79 (s, 1H, N–H), 8.95 (s, 1H, thiazole–H), 12.04 (br.s, 1H, O–H); ^{13}C-NMR (δ ppm): 20.59, 35.50, 108.19, 110.98, 111.46, 112.69, 116.43, 118.14, 122.84, 123.81, 125.20, 129.43, 132.85, 133.30, 138.92, 140.91, 148.32, 158.40, 159.16, 165.74, 170.97, 183.69; elemental microanalysis % for $C_{22}H_{15}N_7O_6S$: calculated/found: 52.28/52.47 (%C), 2.99/3.15 (%H), 19.40/19.68 (%N) and 6.34/6.47 (%S).

*4.1.6.16. 2-Hydroxy-4-{4-[(5-methyoxy-2,3-dioxo-2,3-dihydro-1H-indol-1-yl)methyl]-1H-1,2,3-triazol-1-yl}-N-(5-nitrothiazol-2-yl)benzamide (**5p**).* Reaction time: 4 h; yield: (0.14 g, 82%); m.p.: 165 °C (charring); IR (υ cm^{-1}, KBr): 3396 (O–H), 3274 (N–H), 3146 (Ar–H), 2952 (C–H aliphatic), 1730 (isatin ketonic C═O), 1667 (amidic C═O); ^{1}H-NMR (δ ppm): 3.76 (s, 3H, $-CH_3$), 5.04 (s, 2H, $-CH_2$), 7.10–7.23 (m, 4H, Ar–H), 7.42 (d, J = 7.7 Hz, 1H, Ar–H), 7.49 (s, 1H, triazole–H), 8.05 (d, J = 8.3, 1H, Ar–H), 8.78 (s, 1H, N–H), 8.93 (s, 1H, thiazole–H), 13.69 (br.s, 1H, O–H); ^{13}C-NMR (δ ppm): 35.04, 55.95, 107.66, 109.34, 110.45, 112.21, 117.27, 118.27, 121.91, 123.87, 132.37, 135.64, 140.45, 142.29, 143.28, 143.83, 155.92, 158.00, 158.77, 162.41, 165.64, 183.32; ESI-MS: *m*/*z* calculated for $C_{22}H_{14}N_7O_7S$ $[M-H]^-$:

520.0, found: 520.4; elemental microanalysis % for $C_{22}H_{15}N_7O_7S$: calculated/found: 50.67/50.88 (%C), 2.90/3.14 (%H), 18.80/19.07 (%N) and 6.15/6.08 (%S).

*4.1.6.17. 4-{4-[(Benzo[d]thiazol-2-ylthio)methyl]-1H-1,2,3-triazol-1-yl}-2-hydroxy-N-(5-nitrothiazol-2-yl)benzamide (**5q**).* Reaction time: 2 h; yield: (0.14 g, 86%); m.p.: 255–256 °C (charring); ^{1}H-NMR (δ ppm): 4.81 (s, 2H, –CH_2), 7.38 (t, J = 7.6 Hz, 1H, Ar–H), 7.50 (m, 2H, Ar–H), 7.58 (d, J = 1.9 Hz, 1H, Ar–H), 7.94 (d, J = 8.1 Hz, 1H), 7.96–8.42 (m, 3H, Ar–H and triazole–H), 8.75 (br.s, 1H, N–H), 8.92 (s, 1H, thiazole–H), 12.01 (br.s, 1H, O–H); ^{13}C-NMR (δ ppm): 27.73, 108.33, 111.04, 116.59, 121.79, 122.34, 122.69, 123.01, 125.08, 126.90, 129.34, 132.76, 135.23, 140.85, 144.56, 153.05, 158.35, 159.23, 161.16, 166.01; elemental microanalysis % for $C_{20}H_{13}N_7O_4S_3$: calculated/found: 46.96/47.15 (%C), 2.56/2.67 (%H), 19.17/19.40 (%N) and 18.80/18.59 (%S).

4.2. Biological evaluation

4.2.1. Evaluation of antibacterial activity. According to the CLSI guidelines, the minimum inhibitory concentration of the compounds was determined using the broth micro-dilution method against the wild-type strains of *E. coli* ATCC 8739, *P. aeruginosa* ATCC 27853, *K. pneumoniae* ATCC 10031, *S. aureus* ATCC 6538, and *E. faecalis* ATCC 19433 as well as *H. pylori* ATCC 700392.[83] The investigated bacterial strains were treated with ciprofloxacin as a reference drug for comparison.

4.2.2. Antimycobacterial activity

4.2.2.1. In vitro Mtb MABA assay. In summary, the inoculum was prepared by taking a fresh LJ medium and suspending it in a 7H9-S medium. This 7H9-S medium consisted of 7H9 broth, 0.1% casitone, and 0.5% glycerol, and supplemented with oleic acid, albumin, dextrose, and catalase (OADC). The mixture was adjusted to an OD590 of 1.0 and then diluted at a ratio of 1 : 20. Subsequently, 100 μl of this diluted mixture was used as the inoculum. Resazurin, an indicator for oxidation–reduction (REDOX), underwent a color change as a response to the growth of *Mycobacterium tuberculosis*. This change was quantitatively measured. Each drug's concentrated solution was thawed and diluted in 7H9-S, initially at four times the highest final concentration to be tested. Serial dilutions, progressing in two-fold increments, were directly prepared in a sterile 96-well microtiter plate using 100 μl of 7H9-S. Each plate also had a growth control with no antibiotic and a sterile control. The outer wells contained sterile water to prevent evaporation during incubation. The plates were covered, sealed, and then incubated at 37 °C under normal conditions. After 7 days of incubation, 30 μl of Alamar Blue solution was introduced to each well, followed by another overnight incubation. A color change from blue (oxidized) to pink (reduced) indicated bacterial growth. The minimum inhibitory concentration (MIC) was determined as the lowest drug concentration preventing this color change.[84]

4.2.2.2. In vitro cytotoxicity. Cytotoxicity testing was performed using a mouse macrophage cell line (RAW 264.7) at a concentration of 25 μg mL^{-1}. After 48 hours of exposure, cell viability was assessed based on the conversion of MTT into a formazan product through a cell proliferation assay. The cells were cultivated in RPMI medium supplemented with 10% fetal bovine serum (FBS), 10 000 units of penicillin, and 10 mg of streptomycin per ml in T25 flasks until they reached 80–90% confluency. Subsequently, the cells were seeded at around 5000 cells per well in poly-L-lysine coated plates. The microtiter plates were incubated at 37 °C with 5% CO_2 and 100% relative humidity for 24 hours before introducing the experimental drugs. The test compounds at 25 μg mL^{-1} concentrations were then added and incubated for 48 hours at 37 °C. Following this, 10 μL of a 0.5 mg mL^{-1} MTT solution was added and incubated for 3 hours at 37 °C. The resulting formazan crystals were measured at wavelengths of 595 nm and 625 nm.[84,85]

4.3. Molecular docking simulations

The crystal structures of three proteins were acquired from the Protein Data Bank: pyruvate-ferredoxin oxidoreductase from *Desulfovibrio africanus* (PDB code: 2C42),[86] *E. coli* glucosamine-6-P synthase in complex with glucose-6P and 5-oxo-L-norleucine (PDB code: 2J6H),[87] and *Mycobacterium tuberculosis* dihydrofolate reductase complexed with beta-NADPH and *N*-(4-{[(2-amino-4-oxo-3,4-dihydropteridin-6-yl) methyl]amino}-2-hydroxybenzene-1-carbonyl)-L-glutamic acid (PDB code: 6DDW).[88] These structures were used for docking simulations with the Molecular Operating Environment (MOE 2020.01) software, applying a docking approach that has been used in previous studies.[89,90]

Conflicts of interest

The authors declare no conflicts of interest.

References

1 D. M. Morens, G. K. Folkers and A. S. Fauci, The challenge of emerging and re-emerging infectious diseases, *Nature*, 2004, **430**, 242–249.
2 L. Cantas, S. Q. Shah, L. M. Cavaco, C. M. Manaia, F. Walsh, M. Popowska, H. Garelick, H. Burgmann and H. A. Sorum, A brief multi-disciplinary review on antimicrobial resistance in medicine and its linkage to the global environmental microbiota, *Front. Microbiol.*, 2013, **4**, 96.
3 A. S. Fauci and D. M. Morens, The Perpetual Challenge of Infectious Diseases, *N. Engl. J. Med.*, 2012, **366**, 454–461.
4 J. M. Blair, M. A. Webber, A. J. Baylay, D. O. Ogbolu and L. J. Piddock, Molecular mechanisms of antibiotic resistance, *Nat. Rev. Microbiol.*, 2015, **13**, 42–51.
5 O. Cars, S. J. Chandy, M. Mpundu, A. Q. Peralta, A. Zorzet and A. D. So, Resetting the agenda for antibiotic resistance through a health systems perspective, *Lancet Global Health*, 2021, **9**, e1022–e1027.
6 J. Denissen, B. Reyneke, M. Waso-Reyneke, B. Havenga, T. Barnard, S. Khan and W. Khan, Prevalence of ESKAPE

pathogens in the environment: Antibiotic resistance status, community-acquired infection and risk to human health, *Int. J. Hyg. Environ. Health*, 2022, **244**, 114006.
7 World Health Organization, WHO Consolidated Guidelines on Tuberculosis, Module 5: Management of Tuberculosis in Children and Adolescents, 2022 – **https://apps.who.int**, Geneva, ISBN 978-92-4-004683-2 (electronic version).
8 V. A. Dartois and E. J. Rubin, Anti-tuberculosis treatment strategies and drug development: challenges and priorities, *Nat. Rev. Microbiol.*, 2022, **20**, 685–701.
9 V. Singh and K. Chibale, Strategies to Combat Multi-Drug Resistance in Tuberculosis, *Acc. Chem. Res.*, 2021, **54**, 2361–2376.
10 K. Li, L. A. Schurig-Briccio and X. Feng, *et al.*, Multitarget drug discovery for tuberculosis and other infectious diseases, *J. Med. Chem.*, 2014, **57**, 3126–3139.
11 M. Krátký and J. Vinšová, Salicylanilide Ester Prodrugs as Potential Antimicrobial Agents—A Review, *Curr. Pharm. Des.*, 2011, **17**, 3494–3505.
12 K. Waisser, O. Bures, P. Holy, J. Kunes, R. Oswald, L. Jiraskova, M. Pour, V. Klimesova, L. Kubicova and J. Kaustova, Relationship between the structure and antimycobacterial activity of substituted salicylanilides, *Arch. Pharm.*, 2003, **336**, 53–71.
13 W. A. Hamilton, Mechanism of the Bacteriostatic Action of Tetrachlorosalicylanilide—A Membrane Active Antibacterial Compound, *J. Gen. Microbiol.*, 1968, **50**, 441–458.
14 M. Krátký and J. Vinšová, Antiviral Activity of Substituted Salicylanilides—A Review, *Mini-Rev. Med. Chem.*, 2011, **11**, 956–967.
15 H. Terada, S. Goto, K. Yamamoto, I. Takeuchi, Y. Hamada and K. Miyake, Structural requirements of salicylanilides for uncoupling activity in mitochondria: Quantitative analysis of structure-uncoupling relationships, *Biochim. Biophys. Acta*, 1988, **936**, 504–512.
16 M. J. Macielag, J. P. Demers, S. A. Fraga-Spano, D. J. Hlasta, S. G. Johnson, R. M. Kanojia, R. K. Russel, Z. H. Sui, M. A. Weidner-Wells and H. Werblood, *et al.*, Substituted Salicylanilides as Inhibitors of Two-Component Regulatory Systems in Bacteria, *J. Med. Chem.*, 1998, **41**, 2939–2945.
17 G. A. Dziwornu, H. D. Attram, S. Gachuhi and K. Chibale, Chemotherapy for human schistosomiasis: how far have we come? What's new? Where do we go from here?, *RSC Med. Chem.*, 2020, **11**, 455–490.
18 A. Hemphill, J. Mueller and M. Esposito, Nitazoxanide, a broad-spectrum thiazolide anti-infective agent for the treatment of gastrointestinal infections, *Expert Opin. Pharmacother.*, 2006, **7**, 953–964.
19 B. A. Catto, J. W. Tracy and L. T. Webster Jr, 1-thiocarbamoyl-2-imidazolidinone, a metabolite of niridazole in Schistosoma mansoni, *Mol. Biochem. Parasitol.*, 1984, **10**, 111–120.
20 P. S. Hoffman, G. Sisson, M. A. Croxen, K. Welch, W. D. Harman, N. Cremades and M. G. Morash, Antiparasitic drug nitazoxanide inhibits the pyruvate oxidoreductases of Helicobacter pylori, selected anaerobic bacteria and parasites, and Campylobacter jejuni, *Antimicrob. Agents Chemother.*, 2007, **51**, 868–876.
21 J. L. Blumer, A. Friedman, L. W. Meyer, E. Fairchild, L. T. Webster and W. T. Speck, Relative importance of bacterial and mammalian nitroreductases for niridazole mutagenesis, *Cancer Res.*, 1980, **40**, 4599–4605.
22 J. W. Tracy, B. A. Catto and L. T. Webster, Reductive metabolism of niridazole by adult Schistosoma mansoni. Correlation with covalent drug binding to parasite macromolecules, *Mol. Pharmacol.*, 1983, **24**, 291–299.
23 J. Muller, J. Wastling, S. Sanderson, N. Muller and A. Hemphill, A novel Giardia lamblia nitroreductase, GlNR1, interacts with nitazoxanide and other thiazolides, *Antimicrob. Agents Chemother.*, 2021, **51**, 1979–1986.
24 K. T. Angula, L. J. Legoabe and R. M. Beteck, Chemical classes presenting novel antituberculosis agents currently in different phases of drug development: A 2010–2020 review, *Pharmaceuticals*, 2021, **14**, 461.
25 A. C. White Jr, Nitazoxanide: a new broad spectrum antiparasitic agent, *Expert Rev. Anti-infect. Ther.*, 2004, **2**, 43–49.
26 E. Diaz, J. Mondragon, E. Ramirez and R. Bernal, Epidemiology and control of intestinal parasites with nitazoxanide in children in Mexico, *Am. J. Trop. Med. Hyg.*, 2003, **68**, 384–385.
27 J. C. Chero, M. Saito, J. A. Bustos, E. M. Blanco, G. Gonzalvez and H. H. Garcia, Hymenolepis nana infection: symptoms and response to nitazoxanide in field conditions, *Trans. R. Soc. Trop. Med. Hyg.*, 2007, **101**, 203–205.
28 I. Hagel and T. Giusti, Ascaris lumbricoides: an overview of therapeutic targets, *Infect. Disord.: Drug Targets*, 2010, **10**, 349–367.
29 L. M. Fox and L. D. Saravolatz, Nitazoxanide: a new thiazolide antiparasitic agent, *Clin. Infect. Dis.*, 2005, **40**, 1173–1180.
30 L. Dubreuil, I. Houcke, Y. Mouton and J.-F. Rossignol, In vitro evaluation of activities of nitazoxanide and tizoxanide against anaerobes and aerobic organisms, *Antimicrob. Agents Chemother.*, 1996, **40**, 2266–2270.
31 B. E. Korba, A. B. Montero, K. Farrar, K. Gaye, S. Mukerjee, M. S. Ayers and J.-F. Rossignol, Nitazoxanide, tizoxanide and other thiazolides are potent inhibitors of hepatitis B virus and hepatitis C virus replication, *Antiviral Res.*, 2008, **77**, 56–63.
32 E. B. Keeffe and J.-F. Rossignol, Treatment of chronic viral hepatitis with nitazoxanide and second generation thiazolides, *World J. Gastroenterol.*, 2009, **15**, 1805.
33 L. P. S. de Carvalho, G. Lin, X. Jiang and C. Nathan, Nitazoxanide kills replicating and nonreplicating Mycobacterium tuberculosis and evades resistance, *J. Med. Chem.*, 2009, **52**, 5789–5792.
34 L. P. S. de Carvalho, C. M. Darby, K. Y. Rhee and C. Nathan, Nitazoxanide disrupts membrane potential and intrabacterial pH homeostasis of Mycobacterium tuberculosis, *ACS Med. Chem. Lett.*, 2011, **2**, 849–854.
35 I. S. Adagu, D. Nolder, D. C. Warhurst and J.-F. Rossignol, In vitro activity of nitazoxanide and related compounds against isolates of Giardia intestinalis, Entamoeba histolytica and

Trichomonas vaginalis, *J. Antimicrob. Chemother.*, 2002, **49**, 103–111.

36 J. Broekhuysen, A. Stockis, R. Lins, J. De Graeve and J. Rossignol, Nitazoxanide: pharmacokinetics and metabolism in man, *Int. J. Clin. Pharmacol. Ther.*, 2000, **38**, 387–394.

37 P. S. Hoffman, G. Sisson, M. A. Croxen, K. Welch, W. D. Harman, N. Cremades and M. G. Morash, Antiparasitic drug nitazoxanide inhibits the pyruvate oxidoreductases of Helicobacter pylori, selected anaerobic bacteria and parasites, and Campylobacter jejuni, *Antimicrob. Agents Chemother.*, 2007, **51**, 868–876.

38 G. Sisson, A. Goodwin, A. Raudonikiene, N. J. Hughes, A. K. Mukhopadhyay, D. E. Berg and P. S. Hoffman, Enzymes associated with reductive activation and action of nitazoxanide, nitrofurans, and metronidazole in Helicobacter pylori, *Antimicrob. Agents Chemother.*, 2002, **46**, 2116–2123.

39 J. Müller, J. Wastling, S. Sanderson, N. Müller and A. Hemphill, A novel Giardia lamblia nitroreductase, GlNR1, interacts with nitazoxanide and other thiazolides, *Antimicrob. Agents Chemother.*, 2007, **51**, 1979–1986.

40 J. Müller, A. Naguleswaran, N. Müller and A. Hemphill, Neospora caninum: functional inhibition of protein disulfide isomerase by the broad-spectrum anti-parasitic drug nitazoxanide and other thiazolides, *Exp. Parasitol.*, 2008, **118**, 80–88.

41 J. Odingo, M. A. Bailey, M. Files, J. V. Early, T. Alling, D. Dennison, J. Bowman, S. Dalai, N. Kumar and J. Cramer, In-vitro evaluation of novel nitazoxanide derivatives against Mycobacterium tuberculosis, *ACS Omega*, 2017, **2**, 5873–5890.

42 T. E. Ballard, X. Wang, I. Olekhnovich, T. Koerner, C. Seymour, P. S. Hoffman and T. L. Macdonald, Biological activity of modified and exchanged 2-amino-5-nitrothiazole amide analogues of nitazoxanide, *Bioorg. Med. Chem. Lett.*, 2010, **20**, 3537–3539.

43 T. Ahmed, S. A. Rahman, M. Asaduzzaman, A. B. M. M. K. Islam and A. A. Chowdhury, Synthesis, in vitro bioassays, and computational study of heteroaryl nitazoxanide analogs, *Pharmacol. Res. Perspect.*, 2021, **9**, e00800.

44 4-Aminosalicylic acid, *Tuberculosis*, 2008, 88, 137–138.

45 G. Ramachandran and S. Swaminathan, Safety and tolerability profile of second-line anti-tuberculosis medications, *Drug Saf.*, 2015, **38**, 253–269.

46 D. E. Nawrot, G. Bouz, O. Jand'ourek, K. Konečná, P. Paterová, P. Bárta, M. Novák, R. Kučera, J. Zemanová, M. Forbak, J. Korduláková, O. Pavliš, P. Kubíčková, M. Doležal and J. Zitko, Antimycobacterial pyridine carboxamides: From design to in vivo activity, *Eur. J. Med. Chem.*, 2023, **258**, 115617.

47 S. Rollas and S. G. Küçükgüzel, Biological Activities of Hydrazone Derivatives, *Molecules*, 2007, **12**, 1910–1939.

48 M. Q. Qahtan, E. A. Bakhite, A. M. Sayed, M. Kandeel, D. Sriram and H. H. M. Abdu-Allah, Synthesis, biological evaluation and molecular docking study of some new 4-aminosalicylic acid derivatives as anti-inflammatory and antimycobacterial agents, *Bioorg. Chem.*, 2023, **132**, 106344.

49 H. H. M. Abdu-Allah, B. G. Youssif, M. H. Abdelrahman, M. K. Abdel-Hamid, R. S. Reshma, P. Yogeeswari, T. Aboul-Fadl and D. Sriram, Synthesis and anti-mycobacterial activity of 4-(4-phenyl-1 H-1, 2, 3-triazol-1-yl) salicylhydrazones: revitalizing an old drug, *Arch. Pharmacal Res.*, 2017, **40**, 168–179.

50 P. V. Hegde, M. D. Howe, M. D. Zimmerman, H. I. Boshoff, S. Sharma, B. Remache, Z. Jia, Y. Pan, A. D. Baughn and V. Dartois, Synthesis and biological evaluation of orally active prodrugs and analogs of para-aminosalicylic acid (4-ASA), *Eur. J. Med. Chem.*, 2022, **232**, 114201.

51 R. Tiwari, P. A. Miller, L. R. Chiarelli, G. Mori, M. Šarkan, I. Centárová, S. Cho, K. Mikusova, S. G. Franzblau and A. G. Oliver, Design, syntheses, and anti-TB activity of 1, 3-benzothiazinone azide and click chemistry products inspired by BTZ043, *ACS Med. Chem. Lett.*, 2016, **7**, 266–270.

52 M. D. C. A. D. Bianco, D. I. Leite, F. S. C. Branco, N. Boechat, E. Uliassi, M. L. Bolognesi and M. M. Bastos, The Use of Zidovudine Pharmacophore in Multi-Target-Directed Ligands for AIDS Therapy, *Molecules*, 2022, **27**, 8502.

53 A. M. Jarrad, T. Karoli, A. Debnath, C. Y. Tay, J. X. Huang, G. Kaeslin, A. G. Elliott, Y. Miyamoto, S. Ramu and A. M. Kavanagh, Metronidazole-triazole conjugates: activity against Clostridium difficile and parasites, *Eur. J. Med. Chem.*, 2015, **101**, 96–102.

54 K. Ay, B. Ispartaloğlu, E. Halay, E. Ay, İ. Yaşa and T. Karayıldırım, Synthesis and antimicrobial evaluation of sulfanilamide-and carbohydrate-derived 1, 4-disubstitued-1, 2, 3-triazoles via click chemistry, *Med. Chem. Res.*, 2017, **26**, 1497–1505.

55 S. G. Agalave, S. R. Maujan and V. S. Pore, Click chemistry: 1, 2, 3-triazoles as pharmacophores, *Chem. – Asian J.*, 2011, **6**, 2696–2718.

56 B. Zhang, Comprehensive review on the anti-bacterial activity of 1,2,3-triazole hybrids, *Eur. J. Med. Chem.*, 2019, **168**, 357–372.

57 M. Marinescu, Benzimidazole-Triazole Hybrids as Antimicrobial and Antiviral Agents: A Systematic Review, *Antibiotics*, 2023, **12**, 1220.

58 C. P. Kumar, B. Prathibha, K. Prasad, M. Raghu, M. Prashanth, B. Jayanna, F. A. Alharthi, S. Chandrasekhar, H. Revanasiddappa and K. Y. Kumar, Click synthesis of 1, 2, 3-triazole based imidazoles: Antitubercular evaluation, molecular docking and HSA binding studies, *Bioorg. Med. Chem. Lett.*, 2021, **36**, 127810.

59 Z. Xu, S. Zhang, X. Song, M. Qiang and Z. Lv, Design, synthesis and in vitro anti-mycobacterial evaluation of gatifloxacin-1H-1, 2, 3-triazole-isatin hybrids, *Bioorg. Med. Chem. Lett.*, 2017, **27**, 3643–3646.

60 P. Shanmugavelan, S. Nagarajan, M. Sathishkumar, A. Ponnuswamy, P. Yogeeswari and D. Sriram, Efficient synthesis and in vitro antitubercular activity of 1, 2,

3-triazoles as inhibitors of Mycobacterium tuberculosis, *Bioorg. Med. Chem. Lett.*, 2011, **21**, 7273–7276.
61 S. K. Marvadi, V. S. Krishna, D. Sriram and S. Kantevari, Synthesis of novel morpholine, thiomorpholine and N-substituted piperazine coupled 2-(thiophen-2-yl) dihydroquinolines as potent inhibitors of Mycobacterium tuberculosis, *Eur. J. Med. Chem.*, 2019, **164**, 171–178.
62 M. Yan and S. Ma, Recent advances in the research of heterocyclic compounds as antitubercular agents, *ChemMedChem*, 2012, **7**, 2063–2075.
63 A. Da Settimo, O. Livi, G. Biagi, A. Lucacchini and S. Caselli, 1,2,3-Triazole derivatives of salicylic acid, II, *Farmaco Sci.*, 1983, **38**, 725–737.
64 A. W. Garofalo, S. De Lombaert, J. B. Schwarz, D. Andreotti, F. M. Sabbatini, E. Serra, S. Bernardi, M. Migliore, F. Budassi and C. Beato, Indazoles and azaindazoles as lrrk2 inhibitors, *US Pat.*, US11427558, 2023.
65 J. L. Woodring, R. Behera, A. Sharma, J. Wiedeman, G. Patel, B. Singh, P. Guyett, E. Amata, J. Erath and N. Roncal, Series of alkynyl-substituted thienopyrimidines as inhibitors of protozoan parasite proliferation, *ACS Med. Chem. Lett.*, 2018, **9**, 996–1001.
66 G. Acquaah-Harrison, S. Zhou, J. V. Hines and S. C. Bergmeier, Library of 1, 4-disubstituted 1, 2, 3-triazole analogs of oxazolidinone RNA-binding agents, *J. Comb. Chem.*, 2010, **12**, 491–496.
67 J. Day, M. Uroos, R. A. Castledine, W. Lewis, B. McKeever-Abbas and J. Dowden, Alkaloid inspired spirocyclic oxindoles from 1, 3-dipolar cycloaddition of pyridinium ylides, *Org. Biomol. Chem.*, 2013, **11**, 6502–6509.
68 N. M. Tri, N. D. Thanh, L. N. Ha, D. T. T. Anh, V. N. Toan and N. T. K. Giang, Study on synthesis of some substituted N-propargyl isatins by propargylation reaction of corresponding isatins using potassium carbonate as base under ultrasound- and microwave-assisted conditions, *Chem. Pap.*, 2021, **75**, 4793–4801.
69 A. Oliveira, S. Moura, L. Pimentel, J. Neto, R. Dantas, F. Silva-Jr, M. Bastos and N. Boechat, New imatinib derivatives with antiproliferative activity against A549 and K562 cancer cells, *Molecules*, 2022, **27**, 750.
70 M. R. Aouad, M. A. Soliman, M. O. Alharbi, S. K. Bardaweel, P. K. Sahu, A. A. Ali, M. Messali, N. Rezki and Y. A. Al-Soud, Design, synthesis and anticancer screening of novel benzothiazole-piperazine-1, 2, 3-triazole hybrids, *Molecules*, 2018, **23**, 2788.
71 P. Durand, B. Golinelli-Pimpaneau, S. Mouilleron, B. Badet and M.-A. Badet-Denisot, Highlights of glucosamine-6P synthase catalysis, *Arch. Biochem. Biophys.*, 2008, **474**, 302–317.
72 P. Arora, R. Narang, S. Bhatia, S. K. Nayak, S. K. Singh and B. Narasimhan, Synthesis, molecular docking and QSAR studies of 2, 4-disubstituted thiazoles as antimicrobial agents, *J. Appl. Pharm. Sci.*, 2015, **5**, 28–42.
73 J. Zheng, E. J. Rubin, P. Bifani, V. Mathys, V. Lim, M. Au, J. Jang, J. Nam, T. Dick, J. R. Walker, K. Pethe and L. R. Camacho, para-Aminosalicylic Acid Is a Prodrug Targeting Dihydrofolate Reductase in Mycobacterium tuberculosis, *J. Biol. Chem.*, 2013, **288**, 23447–23456.
74 D. S. Froese, B. Fowler and M. R. Baumgartner, Vitamin B12, folate, and the methionine remethylation cycle—biochemistry, pathways, and regulation, *J. Inherited Metab. Dis.*, 2019, **42**, 673–685.
75 S. Chakraborty, T. Gruber, C. E. B. Barry 3rd, H. I. Boshoff and K. Y. Rhee, Para-Aminosalicylic Acid Acts as an Alternative Substrate of Folate Metabolism in Mycobacterium tuberculosis Sumit, *Science*, 2013, **339**, 88–91.
76 J. Rengarajan, C. M. Sassetti, V. Naroditskaya, A. Sloutsky, B. R. Bloom and E. J. Rubin, Olate pathway is a target for resistance to the drug para-aminosalicylic acid (4-ASA) in mycobacteria, *Mol. Microbiol.*, 2004, **53**, 275–282.
77 I. V. Tetko, A. Yan and J. Gasteiger, Prediction of Physicochemical Properties of Compounds, in *Applied Chemoinformatics: Achievements and Future Opportunities*, ed. T. Engel and J. Gasteiger, 2018, pp. 53–81, Print ISBN:9783527342013|Online ISBN:9783527806539.
78 C. A. Lipinski, F. Lombardo, B. W. Dominy and P. J. Feeney, Experimental and computational approaches to estimate solubility and permeability in drug discovery and development settings, *Adv. Drug Delivery Rev.*, 2001, **46**, 3–26.
79 SwissADME, **http://www.swissadme.ch/index.php**, (accessed 2 July 2023).
80 D. F. Veber, S. R. Johnson, H.-Y. Cheng, B. R. Smith, K. W. Ward and K. D. Kopple, Molecular Properties That Influence the Oral Bioavailability of Drug Candidates, *J. Med. Chem.*, 2002, **45**, 2615–2623.
81 C. A. Lipinski, F. Lombardo, B. W. Dominy and P. J. Feeney, Experimental and computational approaches to estimate solubility and permeability in drug discovery and development settings, *Adv. Drug Delivery Rev.*, 2012, **64**, 4–17.
82 W. A. Holland, Method of making sodium ascorbate, *US Pat.*, US2442005, 1948.
83 H. B. Albada, A.-I. Chiriac, M. Wenzel, M. Penkova, J. E. Bandow, H.-G. Sahl and N. Metzler-Nolte, Modulating the activity of short arginine-tryptophan containing antibacterial peptides with N-terminal metallocenoyl groups, *Beilstein J. Org. Chem.*, 2012, **8**, 1753–1764.
84 L. Collins and S. G. Franzblau, Microplate alamar blue assay versus BACTEC 460 system for high-throughput screening of compounds against Mycobacterium tuberculosis and Mycobacterium avium, *Antimicrob. Agents Chemother.*, 1997, **41**, 1004–1009.
85 V. S. Krishna, S. Zheng, E. M. Rekha, L. W. Guddat and D. Sriram, Discovery and evaluation of novel Mycobacterium tuberculosis ketol-acid reductoisomerase inhibitors as therapeutic drug leads, *J. Comput.-Aided Mol. Des.*, 2019, **33**, 357–366.
86 RCSB PDB, **https://www.rcsb.org/structure/2C42**, (accessed 27 May 2023).

87 RCSB PDB, **https://www.rcsb.org/structure/2J6H**, (accessed 26 May 2023).
88 RCSB PDB, **https://www.rcsb.org/structure/6DDW**, (accessed 1 August 2023).
89 A. A. Alrasheid, M. Y. Babiker and T. A. Awad, Evaluation of certain medicinal plants compounds as new potential inhibitors of novel corona virus (COVID-19) using molecular docking analysis, *In Silico Pharmacol.*, 2021, **9**, 10.
90 A. Mujawah, A. Rauf, S. Bawazeer, A. Wadood, H. A. Hemeg and S. Bawazeer, Isolation, structural elucidation, in vitro anti-α-glucosidase, anti-β-secretase, and in silico studies of bioactive compound isolated from syzygium cumini L, *Processes*, 2023, **11**, 880.

